AIMS Mathematics, 10(5): 10709–10739.
DOI: 10.3934/math.2025487
Received: 06 March 2025
Revised: 16 April 2025
Accepted: 24 April 2025
Published: 09 May 2025

https://www.aimspress.com/journal/Math

Research article

Computational analysis of generalized progressive hybrid log-logistic model and its modeling for physics and engineering applications

Heba S. Mohammed[1], **Osama E. Abo-Kasem**[2] **and Ahmed Elshahhat**[3,*]

[1] Department of Mathematical Sciences, College of Science, Princess Nourah bint Abdulrahman University, P.O. Box 84428, Riyadh 11671, Saudi Arabia

[2] Department of Statistics, Faculty of Commerce, Zagazig University, Zagazig 44519, Egypt

[3] Faculty of Technology and Development, Zagazig University, Zagazig 44519, Egypt

* **Correspondence:** Email: aelshahhat@ftd.zu.edu.eg; Tel: +201225939600.

Abstract: Modern products often have long life cycles and high reliability, making it difficult to collect comprehensive product life data with all unit failures for reliability and quality analysis. So, a new sampling plan called the generalized Type-II progressive hybrid censored strategy has been suggested to minimize test time and costs. This study introduces a novel statistical framework for modeling lifetime data under generalized progressive hybrid censoring using the log-logistic (LogL) lifespan model. Besides traditional methodologies, our approach integrates frequentist and Bayesian inferential techniques to estimate key parameters and reliability metrics, such as the survival and hazard functions of the LogL distribution. The relevant approximate confidence intervals for unknown numbers are also constructed using the frequentest estimators' normal approximations. Incorporating the Markovian technique into Bayesian analysis, we leverage independent gamma priors and the Metropolis-Hastings algorithm to enhance computational efficiency to calculate the Bayes' point estimators along with their highest posterior density interval estimators. Additionally, we propose an optimal progressive censoring scheme that minimizes experimental costs while maintaining estimation accuracy. Extensive Monte Carlo simulations confirm the superiority of the proposed estimators, while three real-world applications in physics and engineering demonstrate their practical efficacy. The findings highlight the versatility of the LogL model and its potential as a robust survival analysis tool under complex real-world conditions.

Keywords: log-logistic; Markovian iterative chain; inference; optimum plan; physics and engineering data modeling
Mathematics Subject Classification: 62F10, 62F15, 62N01, 62N02, 62N05

1. Introduction

Reliability technology, defined as a system's ability to execute its intended process under predetermined conditions for a set amount of time, is becoming increasingly important. Many studies have been conducted in this area. Thus, life-testing studies are frequently carried out in the presence of practical limits such as time and/or cost limitations. Progressive Type-II censoring (PT2C) permits surviving individual(s) to be withdrawn from a test at multiple points; see [1] for details. To establish a PT2C test, at time zero, the experimenter must first put n independent (identical) units into a test, assign the number of target failures m, and assign the progressive (removal) design $\underline{S} = (S_1, S_2, \ldots, S_m)$ such that $n = m + \sum_{i=1}^{m} S_i$. When $X_{1:m:n}$ occurred, S_1 (of $n-1$) units must be taken randomly and removed from the investigation. Similarly, when $X_{2:m:n}$ is noticed, S_2 (of $n - S_1 - 2$) units are removed from the investigation, and so on. Lastly, at $X_{m:m:n}$, all remaining units (say $S_m = n - m - \sum_{j=1}^{m-1} S_j$) are withdrawn.

The primary disadvantage of the PT2C component is that it may take longer to finish the test when the test units are of high quality. Consequently, [2] proposed Type-I progressively hybrid censoring (T1-PHC), which combines PT2C and regular Type-I censoring. Furthermore, a drawback of T1-PHC is that it has a limited amount of failures that may occur before time T, which implies that the estimators produced cannot sometimes be derived. Therefore, [3] proposed progressively Type-II hybrid censoring (T2-PHC). This plan terminates the investigation at $T^* = \max\{X_{m:m:n}, T\}$. Despite the fact that the T2-PHC ensures an efficient quantity of apparent failures, gathering the requisite failures may take some time. As a result, [4] proposed generalized progressive Type-II hybrid censoring (G-T2-PHC). They stated that the experiment under G-T2-PHC is stopped at $T^* = \max\{T_1, \min\{X_{m:m:n}, T_2\}\}$, where the two thresholds $T_i,\ i = 1, 2 (0 < T_1 < T_2)$ and the number $m (1 < m \leq n)$ are prefixed, where d_1 and d_2 represent the total number of failures up to thresholds T_1 and T_2, respectively. If $X_{m:m:n} < T_1$, the investigator will continue to discover failures in a lack of more removals up to T_1 (Case-1), and if $T_1 < X_{m:m:n} < T_2$, they will end the experiment at $X_{m:m:n}$ (Case-2); otherwise, the test will end at T_2 (Case-3). It is vital to note that the G-T2-PHC modifies the T2-PHC by ensuring that the test is completed on time T_2. Thus, T_2 is the longest length of duration that the investigator is willing to permit the test to proceed. So, the investigator will collect one of the following data types:

$$\left.\begin{array}{ll} \text{Case-1:} & \{(X_{1:m:n}, S_1), \ldots, (X_{m-1:m:n}, S_{m-1}), (X_{m:m:n}, 0), \ldots, (X_{d_1:n}, 0)\} \\ \text{Case-2:} & \{(X_{1:m:n}, S_1), \ldots, (X_{d_1:n}, S_{d_1}), \ldots, (X_{m-1:m:n}, S_{m-1}), (X_{m:m:n}, S_m)\} \\ \text{Case-3:} & \{(X_{1:m:n}, S_1), \ldots, (X_{d_1:n}, S_{d_1}), \ldots, (X_{d_2-1:n}, S_{d_2-1}), (X_{d_2:n}, S_{d_2})\} \end{array}\right\} = \{\underline{X}\}.$$

Now, we assume that the variables $\{\underline{X}\}$ represent order lives collected from a continuous population with reliability function (RF) $R(\cdot)$ and probability density function (PDF) $f(\cdot)$. Then, the joint PDF of $\{\underline{X}\}$ is

$$L_\xi(\Omega|\underline{X}) = C_\xi \mathcal{R}_\xi(T_\eta; \Omega) \prod_{j=1}^{D_\xi} f(x_{j:m:n}; \Omega)\Big[R(x_{j:m:n}; \Omega)\Big]^{S_j},\ \xi = 1, 2, 3,\ \eta = 1, 2, \tag{1.1}$$

where Ω is an unknown parametric vector and $\mathcal{S}_\xi(\cdot)$ is a composite form of the RFs under consideration. From (1.1), Table 1 reports the G-T2-PHC notations.

Remark 1: From G-T2-PHC, different sampling strategies can be acquired as special cases, namely:

- T1-PHC (by [2]) if $T_1 \to 0$.

Table 1. The G-T2-PHC notations.

ξ	C_ξ	D_ξ	$\mathcal{R}_\xi(T_\eta;\Omega)$	$S^*_{d_\eta+1}$
1	$\Pi_{j=1}^{d_1}\sum_{i=j}^{m}(S_i+1)$	d_1	$[R(T_1;\Omega)]^{S^*_{d_1+1}}$	$n-d_1-\sum_{i=1}^{m-1}S_i$
2	$\Pi_{j=1}^{m}\sum_{i=j}^{m}(S_i+1)$	m	1	0
3	$\Pi_{j=1}^{d_2}\sum_{i=j}^{m}(S_i+1)$	d_2	$[R(T_2;\Omega)]^{S^*_{d_2+1}}$	$n-d_2-\sum_{i=1}^{d_2}S_i$

- T2-PHC (by [3]) if $T_2 \to \infty$.
- Hybrid-T1 (by [5]) if $T_1 \to 0$, $S_j = 0,\ j = 1, 2, \ldots, m-1$, and $S_m = n - m$.
- Hybrid-T2 (by [6]) if $T_2 \to \infty$, $S_j = 0,\ j = 1, 2, \ldots, m-1$, and $S_m = n - m$.
- Time censoring (by [7]) if $T_1 = 0$, $m = 1$, $S_j = 0,\ j = 1, 2, \ldots, m-1$, and $S_m = n - m$.
- Failure censoring (by [7]) if $T_1 = 0$, $T_2 \to \infty$, $S_j = 0,\ j = 1, 2, \ldots, m-1$, and $S_m = n - m$.

Several investigations have also been completed using G-T2-PHC data. For example, [8] based on the Weibull model, [9] based on the Burr-XII model, [10] based on exponential competing risks, [11] based on the inverted Nadarajah–Haghighi model; [12] based on the Kumaraswamy model, [13] based on the inverted exponentiated-Rayleigh model, and [14, 15] based on alpha-power inverted exponential and Maxwell-Boltzmann distributions, respectively, among others.

The log-logistic (or Fisk) model has been widely used in recent decades to describe time-to-event data, particularly in reliability and econometrics domains; one may refer to [16] for more details. Let X be a random variable that follows the LogL distribution, simply $X \sim \text{LogL}(\gamma, \delta)$, where $\gamma > 0 (\delta > 0)$ is the scale (shape) parameter. Then, its PDF can be defined as:

$$f(x;\gamma,\delta) = \frac{\delta\gamma^\delta x^{\delta-1}}{(x^\delta+\gamma^\delta)^2},\ x > 0. \tag{1.2}$$

Moreover, the RF and HRF of X (at $t > 0$) can be represented as:

$$R(t;\gamma,\delta) = \frac{\gamma^\delta}{t^\delta+\gamma^\delta},\ t > 0, \tag{1.3}$$

and

$$h(t;\gamma,\delta) = \frac{\delta t^{\delta-1}}{t^\delta+\gamma^\delta}, \tag{1.4}$$

respectively. It should be remembered here that, setting $\delta \leqslant 1 (> 1)$ in (1.4), the HRF has a monotonically decreasing (unimodal) shape.

Upon several choices of γ and δ, Figure 1(a) reveals that the LogL density can be positively (or negatively) skewed, unimodal, and bell-shaped, whereas Figure 1(b) indicates that the LogL hazard rate (1.4) has a monotonically decreasing or bathtub-down failure rate shape.

In the reliability literature, based on various censoring scenarios, different efforts have been made to carry out significant studies on the LogL model. For example, [17] for PT2C, [18] for Type-I and Type-II hybrid, [19] for progressive Type-I interval, [20] for adaptive-PT2C, [21] for progressive first-failure, [22] for entropy under PT2C, and [23] for reliability indices under PT2C, among others.

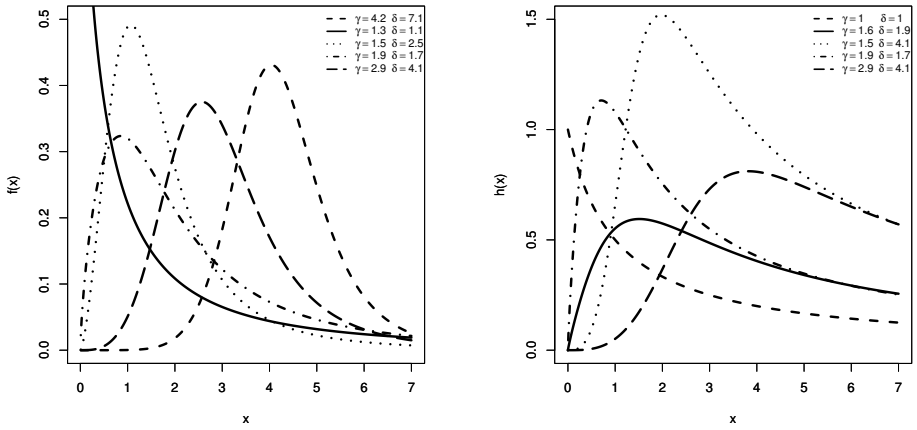

(a) PDF (b) HRF

Figure 1. Several shapes of the LogL's density and hazard rate functions.

The novelty of this study, in the context of imperfect sampling, is that it is the first trial in which likelihood and Bayes frameworks for the LogL distribution's parameters have been compared since its inception. The motivation for this study arises from the proposed generalized censored mechanism's usefulness in enhancing the effectiveness of statistical analysis when compared to its special cases. We have two justifications to perform this study: (1) The LogL distribution's HRF has an inverted bathtub-shaped (or decreasing) form, which is advantageous in many practical applications. (2) The G-T2-PHC plan is beneficial because it allows for the flexibility of stopping trials at a predefined period and reducing overall test length while keeping the desired characteristics of progressive design in practical research. So, far as we are aware, no discussion of inferential elements of the LogL distribution exists, particularly in a reliability context. The purpose of this work, which employs a G-T2-PHC strategy, is to close this gap by demonstrating that the LogL lifetime model may be used as a survival model. As a result, the current study has five contributions, which are as follows:

(1) The problem of estimating the distribution parameters (γ, δ,$R(t)$,$h(t)$) of the LogL model from G-T2-PHC is addressed.
(2) The Bayes estimates of γ, δ, $R(t)$, and $h(t)$ against the squared-error loss (SEL) are assessed using Markov-chain in Monte-Carlo (MCMC) methods using independent gamma conjugate density priors.
(3) In terms of interval estimation, the same unknown parameters are estimated through the approximate confidence interval (ACI) as well as the highest posterior density (HPD) interval.
(4) Since the joint likelihood (or posterior) function of γ and δ cannot be formulated in closed forms, two language packages via R programming software, namely 'maxLik' and 'coda', are recommended.
(5) Find the optimal PT2C based on three popular criteria.
(6) Using a series of Monte Carlo comparisons, the effectiveness of the acquired estimates is evaluated.
(7) From the physical domain, three real-world applications are analyzed to show the LogL

distribution's capacity to fit varied data kinds.

The remaining sections of the study are classified as follows: In Sections 2 and 3, frequentist and Bayes inferences of γ, δ, $R(t)$, and $h(t)$ are obtained, respectively. Section 4 presents different intervals. Simulation outcomes are investigated in Section 5. Section 6 provides the metrics to determine the best censoring design. Three applications are illustrated in Section 7. Ultimately, Section 8 lists some concluding remarks.

2. Likelihood method

Let $\underline{x} = \{x_{j:m:n}, S_j\}$ be a G-T2-PHC data (of size d_2) created from the LogL(γ, δ) population with PDF (1.2) and RF (1.3). Using (1.1), (1.2), and (1.3), where $x_{j:m:n} \cong x_j$ for simplicity, we can write (1.1) up to proportional as

$$L_\xi(\gamma, \delta|\underline{x}) \propto \mathcal{R}_\xi\left(T_\eta; \gamma, \delta\right) \delta^{D_s} \gamma^{\delta\left(D_s + \sum_{j=1}^{D_s} S_j\right)} \prod_{j=1}^{D_s} x_j^{\delta} (x_j^{\delta} + \gamma^{\delta})^{-(S_j+2)}, \tag{2.1}$$

where $\mathcal{R}_1(T_1; \gamma, \delta) = \left[\frac{\gamma^\delta}{T_1^\delta + \gamma^\delta}\right]^{S^*_{d_1+1}}$, $\mathcal{R}_2\left(T_\eta; \gamma, \delta\right) = 1$, and $\mathcal{R}_3(T_2; \gamma, \delta) = \left[\frac{\gamma^\delta}{T_2^\delta + \gamma^\delta}\right]^{S^*_{d_2+1}}$.

The log-likelihood function (say $\ell_\xi \propto L_\xi$) of (2.1) becomes

$$\begin{aligned} \ell_\xi(\gamma, \delta|\underline{x}) \propto \psi_\xi\left(T_\eta; \gamma, \delta\right) + D_s \log(\delta) + \delta(D_s + \sum_{j=1}^{D_s} S_j) \log(\gamma) \\ + \delta \sum_{j=1}^{D_s} \log\left(x_j\right) - \sum_{j=1}^{D_s} \left(S_j + 2\right) \log\left(x_j^\delta + \gamma^\delta\right), \end{aligned} \tag{2.2}$$

where $\psi_\xi\left(T_\eta; \gamma, \delta\right) = \log \mathcal{R}_\xi\left(T_\eta; \gamma, \delta\right)$ for $\xi = 1, 2, 3$, and $\eta = 1, 2$.

The MLEs $\hat{\gamma}$ and $\hat{\delta}$ of γ and δ, respectively, can be acquired from (2.2) as

$$\frac{\partial \ell_\xi}{\partial \gamma} = \psi_\xi^\circ\left(T_\eta; \gamma, \delta\right) + \delta\left[\gamma^{-1}(D_s + \sum_{j=1}^{D_s} S_j) - \gamma^{\delta-1} \sum_{j=1}^{D_s} \left(S_j + 2\right)\left(x_j^\delta + \gamma^\delta\right)^{-1}\right], \tag{2.3}$$

and

$$\begin{aligned} \frac{\partial \ell_\xi}{\partial \delta} = \psi_\xi^\bullet\left(T_\eta; \gamma, \delta\right) + D_s\delta^{-1} + (D_s + \sum_{j=1}^{D_s} S_j) \log(\gamma) + \sum_{j=1}^{D_s} \log\left(x_j\right) \\ - \sum_{j=1}^{D_s} \left(S_j + 2\right)\left(x_j^\delta \log\left(x_j\right) + \gamma^\delta \log(\gamma)\right)\left(x_j^\delta + \gamma^\delta\right)^{-1}, \end{aligned} \tag{2.4}$$

where, for $\xi = 1, 3$ and $\eta = 1, 2$, we have

$\psi_\xi^\circ\left(T_\eta; \gamma, \delta\right) = S^*_{d_\eta+1} \delta\gamma^{-1} T_\eta^\delta \left(T_\eta^\delta + \gamma^\delta\right)^{-1}$,

$\psi_\xi^\circ\left(T_\eta; \gamma, \delta\right) = \psi_\xi^\bullet\left(T_\eta; \gamma, \delta\right) = 0$

and

$\psi_\xi^\bullet\left(T_\eta; \gamma, \delta\right) = S^*_{d_\eta+1} T_\eta^\delta \left(\log(\gamma) - \log\left(T_\eta\right)\right)\left(T_\eta^\delta + \gamma^\delta\right)^{-1}$.

The MLEs of γ and δ must be determined by solving Eqs (2.3) and (2.4) simultaneously using any iterative method. To establish this, we recommend employing iterative numerical optimization techniques such as the Newton-Raphson (N-R) algorithm to get the estimates of $\hat{\gamma}$ and $\hat{\delta}$. To apply this algorithm for evaluating $\hat{\gamma}$ and $\hat{\delta}$ of γ and δ, respectively, based on their functions (2.3) and (2.4), follow the next steps:

Step-1: Set $k = 1$.

Step-2: Set the initial guesses as $(\gamma, \delta) = (\gamma^{(k-1)}, \delta^{(k-1)})$.

Step-3: Compute score values U_γ and U_δ of γ and δ from (2.3) and (2.4), respectively.

Step-4: Compute the Hessian matrix:

$$H = \begin{bmatrix} \frac{\partial^2 \ell_\xi}{\partial \gamma^2} & \frac{\partial^2 \ell_\xi}{\partial \gamma \partial \delta} \\ \frac{\partial^2 \ell_\xi}{\partial \delta \partial \gamma} & \frac{\partial^2 \ell_\xi}{\partial \delta^2} \end{bmatrix}.$$

Step-5: Apply the Newton-Raphson rule:

$$\begin{bmatrix} \gamma^{(k)} \\ \delta^{(k)} \end{bmatrix} = \begin{bmatrix} \gamma^{(k-1)} \\ \delta^{(k-1)} \end{bmatrix} - H^{-1} \begin{bmatrix} U_\gamma \\ U_\delta \end{bmatrix}.$$

Step-6: Stop the iteration (for a small tolerance ϵ) if

$$|\gamma^{(k)} - \gamma^{(k-1)}| < \epsilon \quad \text{and} \quad |\delta^{(k)} - \delta^{(k-1)}| < \epsilon,$$

otherwise, return to Step-3.

Then, the MLEs $\hat{R}(t)$ and $\hat{h}(t)$ can also be produced by substituting γ and δ with their respective $\hat{\gamma}$ or $\hat{\delta}$ as

$$\hat{R}(t) = \frac{\hat{\gamma}^{\hat{\delta}}}{t^{\hat{\delta}} + \hat{\gamma}^{\hat{\delta}}} \quad \text{and} \quad \hat{h}(t) = \frac{\hat{\delta} t^{\hat{\delta}-1}}{t^{\hat{\delta}} + \hat{\gamma}^{\hat{\delta}}},$$

respectively.

3. Bayes method

Instead of evaluating unknown parameter(s) as fixed values (like in classical approaches), using our beliefs about a parameter as we gather more data, the Bayesian setup treats them as random variables with their probability distributions. This framework allows us to combine prior knowledge (knowledge of the parameters before seeing the data) with new evidence (the data) to form a posterior distribution that reflects our updated beliefs. Depending on the SEL function, the Bayes estimators of γ, δ, $R(t)$, and $h(t)$, as well as their related HPD intervals, are produced in this section.

To do this, the LogL parameters γ and δ are assumed to have independent gamma ($Gamma(\cdot)$) priors such as $Gamma(\theta_1, \beta_1)$ and $Gamma(\theta_2, \beta_2)$, respectively. The combined prior density (say, $P(\cdot)$) of γ and δ is

$$P(\gamma, \delta) \propto \gamma^{\theta_1 - 1} \delta^{\theta_2 - 1} e^{-(\gamma \beta_1 + \delta \beta_2)}, \tag{3.1}$$

where $\theta_i > 0$ and $\beta_i > 0$ for $i = 1, 2$, are known. Subsequently, using (2.1) and (3.1), the joint posterior PDF (say $P^*_\xi(\cdot)$) of γ and δ is

$$P^*_\xi(\gamma, \delta | \underline{x}) = \mathcal{K}^{-1} \mathcal{R}_\xi \left(T_\eta; \gamma, \delta \right) \delta^{\theta_2 + D_s - 1} \gamma^{\delta \left(\theta_1 + D_s + \sum_{j=1}^{D_s} S_j \right) - 1}$$

$$\times e^{-(\gamma\beta_1+\delta\beta_2)}\prod_{j=1}^{D_s} x_j^{\delta}(x_j^{\delta}+\gamma^{\delta})^{-(S_j+2)}, \tag{3.2}$$

where $\mathcal{K} = \int_0^\infty \int_0^\infty P(\gamma,\delta)\, L_\xi(\gamma,\delta|\underline{x})\,\mathrm{d}\gamma\mathrm{d}\delta$. Remember that assuming independent gamma priors simplifies modeling by treating each parameter separately, which is especially useful when there is no prior reason to believe that the parameters are related.

It is worth noting here that the proposed gamma distribution as a priori knowledge is often chosen in Bayesian analysis due to: (a) it is flexible and works well for positive parameters like rates; (b) it is conjugate to common likelihoods; (c) its ease of interpretation—the ratio of the shape and rate gives the prior mean; and (d) larger shape values mean more confidence. Additionally, it is flexible enough to be either informative (reflecting strong prior beliefs) or non-informative (letting the data speak more); see [24].

Subsequently, the Bayes' SEL estimate of γ and δ (for short, say $\tilde{\Omega}(\cdot)$) is given by

$$\tilde{\Omega}(\gamma,\delta) = \int_0^\infty \int_0^\infty \Omega(\gamma,\delta)\, P_\xi^*(\gamma,\delta|\underline{x})\mathrm{d}\gamma\mathrm{d}\delta.$$

The entire representation of the marginal density of γ(or δ) is not feasible, as shown by (3.2). As a result, we recommend producing samples from (3.2) using Bayes MCMC algorithms to compute the acquired Bayes estimates and build corresponding HPD intervals. As a result of (3.2), the conditional PDFs ($C_\xi^\gamma(\cdot)$ and $C_\xi^\delta(\cdot)$) of γ and δ are supplied, respectively, as follows:

$$C_\xi^\gamma(\gamma|\delta,\underline{x}) \propto \mathcal{R}_\xi\left(T_\eta;\gamma,\delta\right)\gamma^{\delta\left(\theta_1+D_s+\sum_{j=1}^{D_s}S_j\right)-1}e^{\gamma\beta_1}\prod_{j=1}^{D_s}(x_j^{\delta}+\gamma^{\delta})^{-(S_j+2)} \tag{3.3}$$

and

$$C_\xi^\delta(\delta|\gamma,\underline{x}) \propto \mathcal{R}_\xi\left(T_\eta;\gamma,\delta\right)\delta^{\theta_2+D_s-1}\gamma^{\delta\left(\theta_1+D_s+\sum_{j=1}^{D_s}S_j\right)-1}e^{-\delta\beta_2}\prod_{j=1}^{D_s}x_j^{\delta}(x_j^{\delta}+\gamma^{\delta})^{-(S_j+2)}. \tag{3.4}$$

Obviously, from (3.3) and (3.4), there is no simple way to shrink the posterior distributions of γ and δ to familiar distributions. As a result, the Metropolis-Hastings (M-H) technique is regarded as the best alternative for resolving this problem; for further information, see [25] and [26].

By simulating a single G-T2-PHC dataset (when $(n,m) = (100,50)$ and $(T_1,T_2) = (10,30)$) from the LogL(0.2,0.3), the plots of the conditional PDFs of γ and δ are depicted in Figure 2. It indicates that the posterior PDFs of γ and δ behave similarly to the normal distribution.

So, the M-H steps are:

Step-1: Set the starting values: $\gamma^{(0)} = \hat{\gamma}$ and $\delta^{(0)} = \hat{\delta}$.

Step-2: Set $i = 1$.

Step-3: Simulate $\gamma^\bullet$ from $N(\hat{\gamma},\hat{\sigma}_{\hat{\gamma}}^2)$ and $\delta^\bullet$ from $N(\hat{\delta},\hat{\sigma}_{\hat{\delta}}^2)$.

Step-4: Calculate $\phi_\gamma = \frac{C_\xi^\gamma\left(\gamma^\bullet|\delta^{(i-1)},\underline{x}\right)}{C_\xi^\gamma\left(\gamma^{(i-1)}|\delta^{(i-1)},\underline{x}\right)}$ and $\phi_\delta = \frac{C_\xi^\delta\left(\delta^\bullet|\gamma^{(i)},\underline{x}\right)}{C_\xi^\delta\left(\delta^{(i-1)}|\gamma^{(i)},\underline{x}\right)}$.

Step-5: Create two variates (namely: u_1 and u_2) using the uniform $U(0,1)$ distribution.

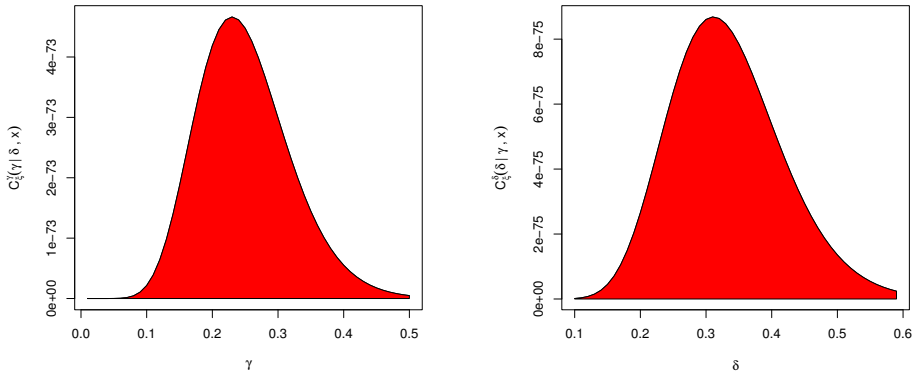

Figure 2. Conditional PDFs of γ (left) and δ (right).

Step-6: Set $\gamma^{(i)} = \gamma^{\bullet}$ and $\delta^{(i)} = \delta^{\bullet}$ if $u_1 < \min\{1, \phi_\gamma\}$ and $u_2 < \min\{1, \phi_\delta\}$. Otherwise, put $\gamma^{(i)} = \gamma^{(i-1)}$ and $\delta^{(i)} = \delta^{(i-1)}$.

Step-7: Set $i = i + 1$.

Step-8: Redo steps 3–7 Q times and ignore the first simulated variated (say $\mathcal{D}$) (burn-in) to get $\gamma^{(i)}$ and $\delta^{(i)}$ for $i = \mathcal{D} + 1, \mathcal{D} + 2, \ldots, Q$.

Step-9: Use $\gamma^{(i)}$ and $\delta^{(i)}$ for $t > 0$ to compute $R(t)$ and $h(t)$, respectively, as

$$R^{(i)}(t) = \frac{\gamma^{(i)^{\delta^{(i)}}}}{t^{\delta^{(i)}} + \gamma^{(i)^{\delta^{(i)}}}} \quad \text{and} \quad h^{(i)}(t) = \frac{\delta^{(i)} t^{\delta^{(i)}-1}}{t^{\delta^{(i)}} + \gamma^{(i)^{\delta^{(i)}}}}.$$

Step-10: Obtain the Bayes' MCMC estimate of γ, δ, $R(t)$, or $h(t)$ (say $\tilde{\Omega}(\cdot)$) as

$$\tilde{\Omega}(\gamma, \delta) = \frac{1}{Q - \mathcal{D}} \sum_{i=\mathcal{D}+1}^{Q} \Omega^{(i)}(\gamma, \delta).$$

4. Interval inference

This part focuses on finding the ACIs (using the observed Fisher's data) and HPD intervals (using simulated Markovian variates) for γ, δ, $R(t)$, and $h(t)$.

4.1. Asymptotic intervals

For creating $100(1 - \epsilon)\%$ ACIs, the asymptotic variance-covariance (AVC) matrix must first be produced by inversely calculating the Fisher's information. Following [27], we derive $\mathbf{I}^{-1}(\cdot)$ as

$$\mathbf{I}^{-1}(\hat{\gamma}, \hat{\delta}) \cong \begin{bmatrix} -l_{11} & -l_{12} \\ -l_{21} & -l_{22} \end{bmatrix}^{-1}_{(\hat{\gamma},\hat{\delta})} = \begin{bmatrix} \hat{\sigma}^2_{\hat{\gamma}} & \hat{\sigma}_{\hat{\gamma}\hat{\delta}} \\ \hat{\sigma}_{\hat{\delta}\hat{\gamma}} & \hat{\sigma}^2_{\hat{\delta}} \end{bmatrix}, \tag{4.1}$$

where

$$l_{11} = \psi_{\xi}^{\circ\circ}\left(T_{\eta};\gamma,\delta\right) - \delta\gamma^{-2}\left(D_s + \sum\nolimits_{j=1}^{D_s} S_j\right) - \left(\delta\left(\gamma^{\delta}+1\right)-1\right)\gamma^{\delta-2}\sum\nolimits_{j=1}^{D_s}\left(S_j+2\right)\left(x_j^{\delta}+\gamma^{\delta}\right)^{-1},$$

$$l_{22} = \psi_{\xi}^{\bullet\bullet}\left(T_{\eta};\gamma,\delta\right) - D_s\delta^{-2} - \sum\nolimits_{j=1}^{D_s}\left(S_j+2\right)\left(x_j^{\delta}+\gamma^{\delta}\right)^{-1}\left[\left(x_j^{\delta}\log^2\left(x_j\right)+\gamma^{\delta}\log^2(\gamma)\right) - \left(x_j^{\delta}\log\left(x_j\right)+\gamma^{\delta}\log(\gamma)\right)^2\left(x_j^{\delta}+\gamma^{\delta}\right)^{-1}\right]$$

and

$$l_{12} = \psi_{\xi}^{\circ\bullet}\left(T_{\eta};\gamma,\delta\right) + \gamma^{-1}\left(D_s + \sum\nolimits_{j=1}^{D_s} S_j\right) - \gamma^{\delta-1}\sum\nolimits_{j=1}^{D_s}\left(S_j+2\right)\left(x_j^{\delta}+\gamma^{\delta}\right)^{-1}\left\{1+\delta\log(\gamma) - \delta\left(x_j^{\delta}\log\left(x_j\right)+\gamma^{\delta}\log(\gamma)\right)\left(x_j^{\delta}+\gamma^{\delta}\right)^{-1}\right\},$$

where

$$\psi_{\xi}^{\circ\circ}\left(T_{\eta};\gamma,\delta\right) = -S^{*}_{d_{\eta}+1}\delta\gamma^{-2}T_{\eta}^{\delta}\left(T_{\eta}^{\delta}+\gamma^{\delta}\right)^{-1}\left[1+\delta\gamma^{\delta}\left(T_{\eta}^{\delta}+\gamma^{\delta}\right)^{-1}\right],$$

$$\psi_{\xi}^{\bullet\bullet}\left(T_{\eta};\gamma,\delta\right) = S^{*}_{d_{\eta}+1}T_{\eta}^{\delta}\left(\log(\gamma)-\log\left(T_{\eta}\right)\right)\left(T_{\eta}^{\delta}+\gamma^{\delta}\right)^{-1} \times\left[\log\left(T_{\eta}\right) - \left(T_{\eta}^{\delta}\log\left(T_{\eta}\right)+\gamma^{\delta}\log(\gamma)\right)\left(T_{\eta}^{\delta}+\gamma^{\delta}\right)^{-1}\right]$$

and

$$\psi_{\xi}^{\circ\bullet}\left(T_{\eta};\gamma,\delta\right) = S^{*}_{d_{\eta}+1}\gamma^{-1}T_{\eta}^{\delta}\left(T_{\eta}^{\delta}+\gamma^{\delta}\right)^{-1}\left[1-\delta\gamma^{\delta}\left(\log(\gamma)-\log\left(T_{\eta}\right)\right)\left(T_{\eta}^{\delta}+\gamma^{\delta}\right)^{-1}\right].$$

Thus, the respective $100(1-\epsilon)\%$ ACIs of γ and δ are provided by

$$\hat{\gamma} \mp z_{\frac{\epsilon}{2}}\sqrt{\hat{\sigma}^2_{\hat{\gamma}}} \quad \text{and} \quad \hat{\delta} \mp z_{\frac{\epsilon}{2}}\sqrt{\hat{\sigma}^2_{\hat{\delta}}},$$

where $z_{\frac{\epsilon}{2}}$ denotes the top $\frac{\epsilon}{2}$ percentage points of the standard Gaussian distribution.

To build the ACI of $R(t)$ (or $h(t)$), the delta idea is re-utilized to get the estimated variances $\hat{\sigma}^2_{\hat{R}(t)}$ and $\hat{\sigma}^2_{\hat{h}(t)}$ of $\hat{R}(t)$ and $\hat{h}(t)$ (see [28]) as

$$\hat{\sigma}^2_{\hat{R}(t)} = \mho_{\hat{R}}^{\mathsf{T}}\mathbf{I}^{-1}\left(\hat{\gamma},\hat{\delta}\right)\mho_{\hat{R}} \quad \text{and} \quad \hat{\sigma}^2_{\hat{h}(t)} = \mho_{\hat{h}}^{\mathsf{T}}\mathbf{I}^{-1}\left(\hat{\gamma},\hat{\delta}\right)\mho_{\hat{h}},$$

respectively, where $\mho_{\hat{R}}^{\mathsf{T}} = \left[\frac{\partial R(t)}{\partial\gamma} \quad \frac{\partial R(t)}{\partial\delta}\right]_{(\hat{\gamma},\hat{\delta})}$ and $\mho_{\hat{h}}^{\mathsf{T}} = \left[\frac{\partial h(t)}{\partial\gamma} \quad \frac{\partial h(t)}{\partial\delta}\right]_{(\hat{\delta},\hat{\gamma})}$.

So, the $100(1-\epsilon)\%$ ACIs of $R(t)$ and $h(t)$ are respectively provided by

$$\hat{R}(t) \mp z_{\frac{\epsilon}{2}}\sqrt{\hat{\sigma}^2_{\hat{R}(t)}} \quad \text{and} \quad \hat{h}(t) \mp z_{\frac{\epsilon}{2}}\sqrt{\hat{\sigma}^2_{\hat{h}(t)}}.$$

4.2. HPD intervals

To create an HPD interval estimator of γ, δ, $R(t)$, or $h(t)$ (say Ω), following the technique proposed by [29], we first rank the simulated MCMC samples (developed in Section 3) of $\Omega^{(i)}$ for $i = \mathcal{D}+1, \mathcal{D}+2, \ldots, Q$ as $\Omega_{(Q_0+1)}, \Omega_{(Q_0+2)}, \ldots, \Omega_{(Q)}$. Hence, the $100(1-\epsilon)\%$ HPD interval of Ω is

$$\Omega_{(i^*)}, \Omega_{(i^*+(1-\epsilon)(Q-\mathcal{D}))},$$

where $i^* = \mathcal{D}+1, \mathcal{D}+2, \ldots, Q$ is specified as

$$\Omega_{(i^*+[(1-\epsilon)(Q-\mathcal{D})])} - \Omega_{(i^*)} = \min_{1 \leqslant i \leqslant \epsilon(Q-\mathcal{D})} \left[\Omega_{(i+[(1-\epsilon)(Q-\mathcal{D})])} - \Omega_{(i)}\right].$$

5. Monte Carlo simulations

To demonstrate the true performance of the offered point (or interval) estimators of γ, δ, $R(t)$, or $h(t)$, based on different options of $T_i, i = 1, 2$, n, m, and $\underline{S}$, several simulations are conducted. To establish this objective, from LogL(0.5, 1.5), we replicate the G-T2-PHC strategy 1000 times. Taking $t = 0.25$, the true value of $(R(t), h(t))$ is taken as (0.7101,0.5798). Further, taking n(=50,80) and $(T_1, T_2) = (1, 2)$ and (2,5), the level of m is taken as a failure percent (FP%), such as $\frac{m}{n}$(=40,80)%. Various censoring designs $\underline{S}$ are also provided, namely,

$$\begin{aligned}
&\text{Scheme-1}: \ \underline{S} = \left(n-m, 0^{m-1}\right),\\
&\text{Scheme-2}: \ \underline{S} = \left(0^{\frac{m}{2}-1}, n-m, 0^{\frac{m}{2}}\right),\\
&\text{Scheme-3}: \ \underline{S} = \left(0^{m-1}, n-m\right),
\end{aligned}$$

where $\underline{S} = (1, 0, 0, 3)$ (for example) is denoted as $\underline{S} = (1, 0^2, 3)$.

Once 1000 G-T2-PHC samples are collected, by installing the 'maxLik' package (by [30]) in R, the MLEs and 95% ACI estimates of γ, δ, $R(t)$, or $h(t)$ are obtained via an N-R iterative sampler. The initial guess points used in this iterative method are taken as the actual values of LogL(γ, δ) proposed in this part.

To carry out the Bayes' inference, by installing the 'coda' package (by [31]) in R, 12,000 MCMC samples are generated, and the first 2,000 iterations are ignored as burn-in. We now follow Kundu's [32] idea to determine the values of the hyper-parameters (θ_i, β_i), $i = 1, 2$. Following the mean and variance associated with the proposed gamma priors, two sets are considered, namely:

- Prior-1 (P1): $(\theta_1, \theta_2) = (2.5, 7.5)$ and $\beta_i = 5, \ i = 1, 2$;
- Prior-2 (P2): $(\theta_1, \theta_2) = (5, 15)$ and $\beta_i = 10, \ i = 1, 2$.

To examine the validity and efficiency status of the collected 12,000 iterations of γ, δ, $R(t)$, or $h(t)$ produced from the proposed Bayes MCMC sampler, using Scheme-1, Prior-1, $(T_1, T_2) = (1, 2)$, and n[FP%] = 50[40%] (as an example), three tools for visualizing the convergence of MCMC draws are used, namely:

(1) Autocorrelation function (ACF) plot: It shows how much each sample in the chain differs from the previous one. To put it another way, it indicates the degree of serial correlation between the draws.

(2) Brooks-Gelman-Rubin (BGR) plot: It evaluates an MCMC's chain convergence by comparing the variances within/between Markovian chains.
(3) Trace (with thinning) plot: It displays the sampled values for each chain and node during the series of iterations.

To display these plots, we take every fourth point (for example) from a total of 12,000 MCMC variables collected from the posterior of γ and δ, see Figure 3. Figure 3(a) shows that the sample autocorrelation between the terms of the chain decreases as a function of their lag, thus the acquired estimates for the acquired point (or interval) estimates of γ, δ, $R(t)$, or $h(t)$ become more reliable; Figure 3(b) indicates there is no difference among the variances within and between simulated chains; Figure 3(c) emphasizes that the collected MCMC iterations are suitably mixed and that the duration of the draws discarded at the beginning of each chain is adequate to decrease autocorrelation. Thus, the quality of MCMC evaluations is adequate to offer a precise estimate of the target distribution.

Specifically, the average estimates (Av.Es) of γ (for instance) are given by

$$\text{Av.E}(\check{\gamma}) = \frac{1}{1000}\sum\nolimits_{i=1}^{1000}\check{\gamma}^{(i)},$$

where $\check{\gamma}^{(i)}$ is the calculated estimate of γ at the ith sample.

The root mean squared errors (RMSEs) and mean relative absolute biases (MRABs) for the point estimates of γ are compared as

$$\text{RMSE}(\check{\gamma}) = \sqrt{\frac{1}{1000}\sum\nolimits_{i=1}^{1000}\left(\check{\gamma}^{(i)}-\gamma\right)^2},$$

and

$$\text{MRAB}(\check{\gamma}) = \frac{1}{1000}\sum\nolimits_{i=1}^{1000}\frac{1}{\gamma}\left|\check{\gamma}^{(i)}-\gamma\right|,$$

respectively.

Moreover, to compare the acquired interval estimates of γ, we consider two criteria, namely, average confidence lengths (ACLs) and coverage percentages (CPs) as

$$\text{ACL}_{(1-\epsilon)\%}(\gamma) = \frac{1}{1000}\sum\nolimits_{i=1}^{1000}\left(\mathcal{U}_{\check{\gamma}^{(i)}}-\mathcal{L}_{\check{\gamma}^{(i)}}\right),$$

and

$$\text{CP}_{(1-\epsilon)\%}(\gamma) = \frac{1}{1000}\sum\nolimits_{i=1}^{1000}\mathbf{1}^{\star}_{\left(\mathcal{L}_{\check{\gamma}^{(i)}};\mathcal{U}_{\check{\gamma}^{(i)}}\right)}(\gamma),$$

respectively, where $\mathbf{1}^{\star}(\cdot)$ is an indicator, and $(\mathcal{L}(\cdot),\mathcal{U}(\cdot))$ denotes the (lower,upper) limits of the $(1-\epsilon)\%$ interval of γ.

From Tables 2–9, in terms of the smallest RMSE, MRAB, and ACL values, as well as the largest CP values, we report the following facts:

- The acquired classical (or Bayes) estimates of γ, δ, $R(t)$, or $h(t)$ show good performance; that is, the main general note.
- As n (or FP%) grows, all offered estimates of γ, δ, $R(t)$, or $h(t)$ perform better. A similar conclusion is obtained when $n-m$ decreases.

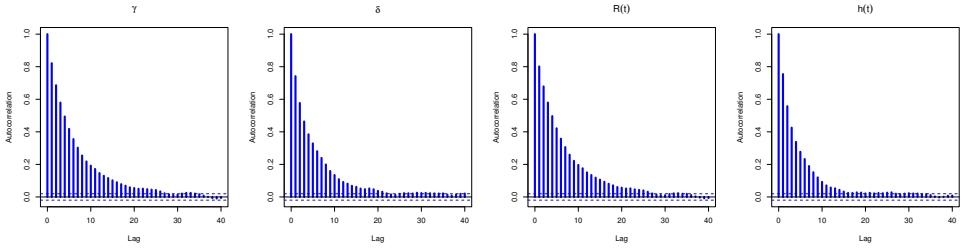

(a) ACF

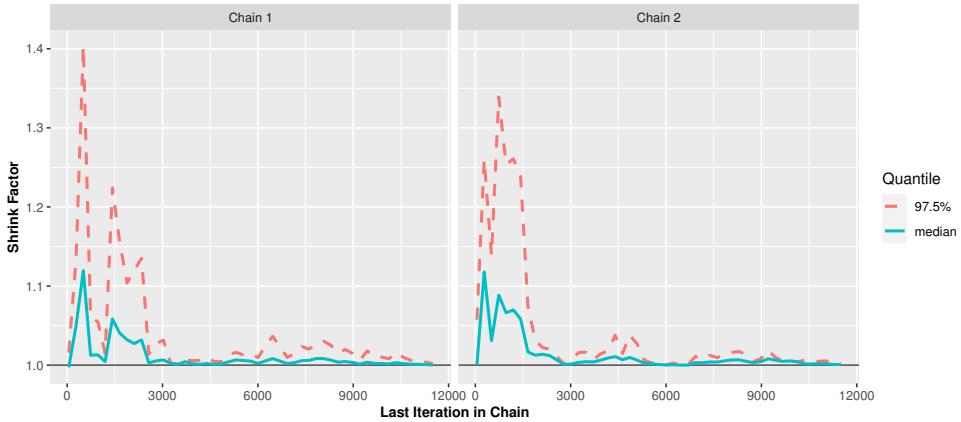

(b) BGR

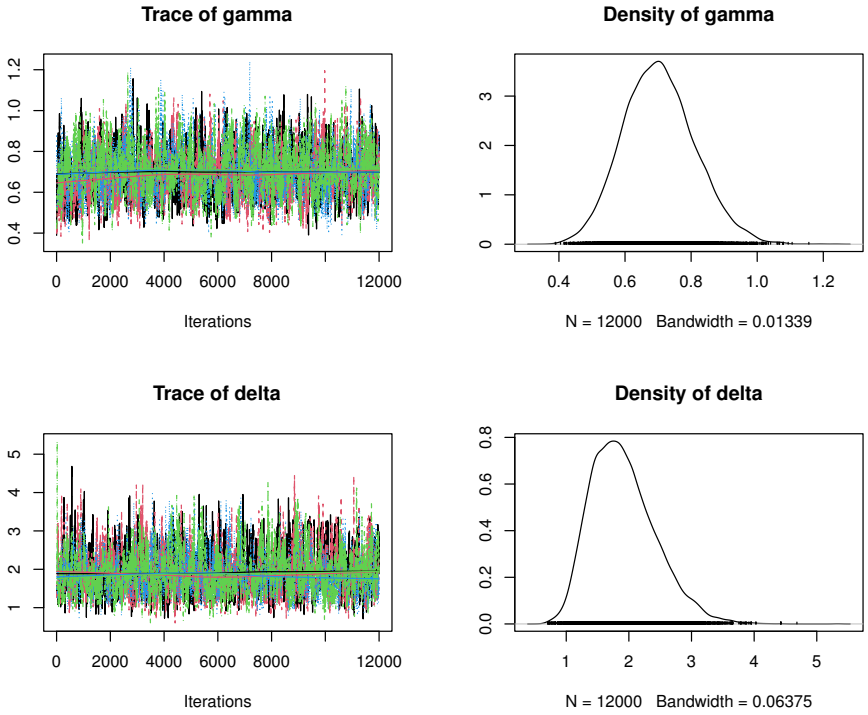

(c) Trace

Figure 3. The ACF, BGR, and Trace diagrams for γ, δ, $R(t)$, and $h(t)$ in Monte Carlo simulation.

- The MCMC estimates of all considered parameters, due to the priority of gamma information, behave well compared to those developed by others. A similar comment is also reached for HPD interval estimates.
- Because the variation in Prior-2 is comparatively lower than in Prior-1, for all unknown parameters, MCMC analysis based on the prior provides more efficient estimates compared to the others.
- As $T_i,\ i = 1, 2$, grow, it is noted that:
  - The RMSE, MRAB, and ACL of γ, $R(t)$, and $h(t)$ decrease, whereas their CPs grow.
  - The RMSE, MRAB, and ACL of δ grow, while their CPs decrease.
- Comparing $\underline{\mathrm{S}}$: 1, 2, and 3, it is observed that the estimates of γ, δ, $R(t)$, and $h(t)$ behave well based on Scheme-3 'right-censoring'.
- As a consequence, in the presence of data produced via a generalized Type-II progressively hybrid mechanism, the Bayes Metropolis-Hastings-based methodology is recommended.

Table 2. The Av.Es (1^{st} column), RMSEs (2^{nd} column), and MRABs (3^{rd} column) of γ.

(T_1, T_2)	n[FP%]	Scheme	MLE			MCMC					
Prior →						P1			P2		
(1,2)	50[40%]	1	0.6613	0.3189	0.2965	0.7961	0.1929	0.1725	0.5925	0.1883	0.1642
		2	0.6535	0.2950	0.2751	0.6094	0.1874	0.1598	0.5727	0.1740	0.1565
		3	0.6462	0.2263	0.2047	0.7034	0.1843	0.1561	0.5881	0.1534	0.1402
	50[80%]	1	0.6003	0.2129	0.1918	0.6626	0.1790	0.1503	0.5747	0.1237	0.1239
		2	0.5952	0.1867	0.1647	0.5578	0.1681	0.1476	0.5605	0.1102	0.1019
		3	0.5911	0.1573	0.1393	0.6233	0.1500	0.1286	0.5709	0.1016	0.0925
	80[40%]	1	0.6659	0.1477	0.1160	0.7751	0.1316	0.1067	0.6725	0.0969	0.0887
		2	0.6461	0.1327	0.1083	0.5885	0.1177	0.0978	0.6402	0.0920	0.0815
		3	0.6380	0.1237	0.1012	0.6914	0.0959	0.0892	0.6598	0.0843	0.0747
	80[80%]	1	0.5991	0.1183	0.0991	0.4974	0.0851	0.0727	0.6038	0.0703	0.0575
		2	0.5892	0.1121	0.0949	0.4572	0.0806	0.0686	0.5884	0.0652	0.0524
		3	0.5925	0.1102	0.0930	0.4909	0.0697	0.0605	0.6018	0.0600	0.0488
(2,5)	50[40%]	1	0.6379	0.2853	0.2651	0.7646	0.1708	0.1568	0.5889	0.1681	0.1417
		2	0.6317	0.2321	0.2118	0.5708	0.1669	0.1461	0.5651	0.1590	0.1370
		3	0.6223	0.1918	0.1699	0.6679	0.1619	0.1423	0.5837	0.1555	0.1267
	50[80%]	1	0.5819	0.1553	0.1371	0.5397	0.1437	0.1240	0.5511	0.1236	0.1096
		2	0.5772	0.1468	0.1256	0.5365	0.1382	0.1186	0.5516	0.1098	0.1019
		3	0.5739	0.1359	0.1186	0.5680	0.1144	0.0985	0.5600	0.0975	0.0894
	80[40%]	1	0.6399	0.1124	0.0902	0.7115	0.0999	0.0872	0.6568	0.0945	0.0814
		2	0.6232	0.1091	0.0874	0.6155	0.0926	0.0817	0.6461	0.0826	0.0765
		3	0.6162	0.1058	0.0846	0.6205	0.0858	0.0763	0.6423	0.0745	0.0651
	80[80%]	1	0.5807	0.0999	0.0832	0.4799	0.0691	0.0600	0.5898	0.0595	0.0548
		2	0.5725	0.0973	0.0794	0.4876	0.0639	0.0565	0.5957	0.0591	0.0499
		3	0.5749	0.0925	0.0770	0.4754	0.0604	0.0511	0.5871	0.0565	0.0460

Table 3. The Av.Es (1^{st} column), RMSEs (2^{nd} column), and MRABs (3^{rd} column) of δ.

(T_1, T_2)	n[FP%]	Scheme	MLE			MCMC					
Prior →						P1			P2		
(1,2)	50[40%]	1	1.3383	1.8502	1.2611	1.4138	1.4318	1.2069	1.5180	0.9832	0.8869
		2	1.2074	1.7136	1.2354	1.2783	1.3737	0.9346	1.5164	0.9592	0.8383
		3	1.1858	1.4885	1.2055	1.6581	1.3410	0.8334	1.5166	0.9333	0.8083
	50[80%]	1	1.3914	1.3722	1.1134	1.7195	1.2467	0.7835	1.5230	0.8192	0.7187
		2	1.5043	1.2820	1.0950	1.5574	1.2231	0.7509	1.5249	0.7917	0.6987
		3	1.3612	1.1992	1.0645	1.6533	1.1564	0.7361	1.5210	0.7841	0.6823
	80[40%]	1	1.7055	1.0799	1.0043	1.8307	1.0657	0.7199	1.5883	0.4399	0.4921
		2	1.7354	0.9559	0.8914	1.1673	0.9437	0.6730	1.5829	0.3898	0.3595
		3	1.5645	0.9192	0.8612	1.5950	0.8283	0.6434	1.5834	0.3757	0.3278
	80[80%]	1	1.5950	0.8954	0.8383	1.6278	0.7873	0.5416	1.5679	0.3626	0.2970
		2	1.7961	0.7697	0.7074	1.5006	0.7403	0.5286	1.5711	0.3490	0.2622
		3	1.6134	0.7495	0.6858	1.5796	0.6701	0.4966	1.5674	0.3386	0.2535
(2,5)	50[40%]	1	2.1880	1.9710	1.3755	1.3555	1.5197	1.1791	1.5172	1.0021	0.9006
		2	1.3956	1.8583	1.2901	1.3095	1.4751	0.9754	1.5165	0.9932	0.8897
		3	1.8109	1.6591	1.2795	1.2992	1.4146	0.8936	1.5164	0.9701	0.8655
	50[80%]	1	1.8041	1.4039	1.2757	1.5632	1.2320	0.7931	1.5249	0.8746	0.7936
		2	1.6439	1.3778	1.1493	1.5334	1.2186	0.7673	1.5241	0.8433	0.7482
		3	1.7272	1.2498	1.1216	1.4864	1.1582	0.7423	1.5232	0.8148	0.7132
	80[40%]	1	2.0147	1.2145	1.0632	1.8755	1.1242	0.7145	1.5897	0.3969	0.3292
		2	1.2825	1.0434	1.0334	1.6216	1.0938	0.6992	1.5886	0.3832	0.3041
		3	1.7255	0.9543	0.9864	1.7757	0.8615	0.6519	1.5861	0.3788	0.2854
	80[80%]	1	1.7312	0.9135	0.8555	1.7795	0.8007	0.5676	1.5774	0.3571	0.2813
		2	1.5727	0.8825	0.8095	1.6493	0.7650	0.5454	1.5705	0.3437	0.2670
		3	1.6762	0.8595	0.7992	1.7901	0.6595	0.4875	1.5716	0.3346	0.2498

Table 4. The Av.Es (1^{st} column), RMSEs (2^{nd} column), and MRABs (3^{rd} column) of $R(t)$.

(T_1, T_2)	n[FP%]	Scheme	MLE			MCMC					
Prior →						P1			P2		
(1,2)	50[40%]	1	0.7507	0.1503	0.1471	0.8514	0.0833	0.0880	0.7441	0.0706	0.0652
		2	0.6971	0.1461	0.1413	0.7877	0.0812	0.0764	0.7372	0.0658	0.0608
		3	0.7229	0.1211	0.1173	0.8179	0.0790	0.0637	0.7425	0.0593	0.0545
	50[80%]	1	0.7352	0.1129	0.1078	0.8138	0.0748	0.0605	0.7384	0.0449	0.0416
		2	0.7248	0.1093	0.1037	0.7808	0.0663	0.0543	0.7335	0.0441	0.0408
		3	0.7269	0.0953	0.0893	0.7993	0.0632	0.0515	0.7369	0.0397	0.0366
	80[40%]	1	0.7605	0.0927	0.0879	0.8572	0.0608	0.0495	0.7753	0.0375	0.0340
		2	0.6985	0.0838	0.0777	0.7980	0.0606	0.0493	0.7646	0.0358	0.0324
		3	0.7334	0.0783	0.0713	0.8274	0.0598	0.0484	0.7709	0.0340	0.0308
	80[80%]	1	0.7397	0.0615	0.0518	0.7580	0.0541	0.0467	0.7516	0.0327	0.0291
		2	0.7278	0.0598	0.0468	0.7470	0.0508	0.0415	0.7466	0.0306	0.0268
		3	0.7340	0.0536	0.0462	0.7557	0.0468	0.0392	0.7509	0.0271	0.0234
(2,5)	50[40%]	1	0.7557	0.1384	0.1386	0.8437	0.0810	0.0865	0.7428	0.0653	0.0604
		2	0.7030	0.1279	0.1236	0.7782	0.0790	0.0816	0.7345	0.0615	0.0569
		3	0.7288	0.1171	0.1168	0.8117	0.0763	0.0761	0.7410	0.0602	0.0554
	50[80%]	1	0.7367	0.1060	0.1014	0.7760	0.0729	0.0694	0.7302	0.0421	0.0390
		2	0.7263	0.0988	0.0943	0.7738	0.0666	0.0609	0.7304	0.0401	0.0371
		3	0.7287	0.0809	0.0745	0.7843	0.0650	0.0550	0.7333	0.0391	0.0361
	80[40%]	1	0.7652	0.0780	0.0684	0.8440	0.0625	0.0497	0.7705	0.0362	0.0327
		2	0.7044	0.0739	0.0665	0.8044	0.0598	0.0483	0.7670	0.0343	0.0309
		3	0.7388	0.0715	0.0644	0.8115	0.0588	0.0464	0.7655	0.0281	0.0244
	80[80%]	1	0.7412	0.0580	0.0488	0.7566	0.0540	0.0444	0.7471	0.0267	0.0232
		2	0.7290	0.0541	0.0444	0.7559	0.0506	0.0414	0.7490	0.0249	0.0203
		3	0.7357	0.0501	0.0419	0.7550	0.0475	0.0386	0.7462	0.0238	0.0181

Table 5. The Av.Es (1^{st} column), RMSEs (2^{nd} column), and MRABs (3^{rd} column) of $h(t)$.

(T_1, T_2)	n[FP%]	Scheme	MLE			MCMC					
Prior →						P1			P2		
(1,2)	50[40%]	1	0.6687	0.3705	0.2660	0.4567	0.1619	0.1464	0.6039	0.1000	0.1204
		2	0.8025	0.3069	0.2348	0.5078	0.1338	0.1231	0.5999	0.0981	0.1178
		3	0.7257	0.2990	0.2137	0.5001	0.1294	0.1216	0.6033	0.0856	0.1005
	50[80%]	1	0.6343	0.2632	0.1928	0.4818	0.1272	0.1115	0.5992	0.0825	0.0970
		2	0.6530	0.2235	0.1681	0.4794	0.1240	0.1107	0.5956	0.0806	0.0942
		3	0.6447	0.1960	0.1477	0.4897	0.1152	0.1052	0.5986	0.0760	0.0891
	80[40%]	1	0.6424	0.1778	0.1345	0.4335	0.1134	0.1035	0.5964	0.0740	0.0863
		2	0.7862	0.1767	0.1323	0.4694	0.1047	0.1004	0.5970	0.0736	0.0858
		3	0.6876	0.1720	0.1309	0.4698	0.1040	0.0980	0.5976	0.0733	0.0853
	80[80%]	1	0.6223	0.1344	0.1031	0.4767	0.0955	0.0901	0.5970	0.0716	0.0830
		2	0.6401	0.1311	0.1013	0.4582	0.0889	0.0797	0.5941	0.0697	0.0789
		3	0.6293	0.1280	0.0991	0.4749	0.0783	0.0720	0.5968	0.0626	0.0717
(2,5)	50[40%]	1	0.6298	0.3286	0.2315	0.4636	0.1603	0.1431	0.6033	0.0981	0.1177
		2	0.7597	0.2869	0.1996	0.4975	0.1316	0.1188	0.5981	0.0947	0.1131
		3	0.6831	0.2605	0.1866	0.4913	0.1264	0.1183	0.6024	0.0790	0.0998
	50[80%]	1	0.6107	0.2288	0.1680	0.4744	0.1240	0.1172	0.5931	0.0763	0.0934
		2	0.6296	0.1905	0.1450	0.4769	0.1215	0.1162	0.5934	0.0741	0.0877
		3	0.6213	0.1705	0.1324	0.4813	0.1189	0.1081	0.5957	0.0710	0.0826
	80[40%]	1	0.6045	0.1657	0.1181	0.4350	0.1170	0.1065	0.5963	0.0704	0.0797
		2	0.7430	0.1570	0.1168	0.4755	0.1084	0.1051	0.5963	0.0676	0.0785
		3	0.6496	0.1533	0.1164	0.4611	0.1060	0.1029	0.5965	0.0634	0.0731
	80[80%]	1	0.5995	0.1168	0.0985	0.4626	0.1021	0.0897	0.5944	0.0615	0.0707
		2	0.6190	0.1149	0.0943	0.4718	0.0955	0.0885	0.5955	0.0601	0.0679
		3	0.6066	0.1135	0.0888	0.4615	0.0868	0.0823	0.5939	0.0572	0.0646

Table 6. The ACLs (1^{st} column) and CPs (2^{nd} column), of 95% ACI/HPD intervals of γ.

(T_1, T_2)	n[FP%]	Scheme	ACI		HPD			
Prior →					P1		P2	
(1,2)	50[40%]	1	0.554	0.929	0.482	0.940	0.238	0.952
		2	0.544	0.931	0.410	0.943	0.218	0.954
		3	0.529	0.934	0.390	0.946	0.197	0.957
	50[80%]	1	0.443	0.938	0.359	0.950	0.158	0.961
		2	0.425	0.939	0.333	0.951	0.151	0.962
		3	0.412	0.941	0.325	0.953	0.145	0.965
	80[40%]	1	0.407	0.943	0.313	0.955	0.138	0.967
		2	0.396	0.945	0.297	0.957	0.131	0.968
		3	0.362	0.948	0.278	0.960	0.128	0.972
	80[80%]	1	0.330	0.951	0.228	0.963	0.127	0.975
		2	0.325	0.952	0.219	0.964	0.116	0.977
		3	0.306	0.953	0.209	0.967	0.109	0.978
(2,5)	50[40%]	1	0.518	0.934	0.427	0.945	0.215	0.957
		2	0.484	0.936	0.386	0.947	0.199	0.959
		3	0.467	0.939	0.358	0.950	0.179	0.962
	50[80%]	1	0.415	0.941	0.313	0.953	0.149	0.964
		2	0.382	0.944	0.295	0.955	0.138	0.967
		3	0.363	0.946	0.287	0.958	0.132	0.969
	80[40%]	1	0.362	0.948	0.281	0.960	0.129	0.970
		2	0.359	0.950	0.278	0.962	0.126	0.973
		3	0.354	0.951	0.271	0.963	0.121	0.975
	80[80%]	1	0.313	0.955	0.236	0.967	0.118	0.980
		2	0.282	0.957	0.215	0.969	0.114	0.981
		3	0.268	0.961	0.205	0.970	0.107	0.982

Table 7. The ACLs (1^{st} column) and CPs (2^{nd} column), of 95% ACI/HPD intervals of δ.

(T_1, T_2)	n[FP%]	Scheme	ACI		HPD			
Prior →					P1		P2	
(1,2)	50[40%]	1	3.096	0.869	1.902	0.895	0.837	0.908
		2	2.809	0.884	1.838	0.897	0.799	0.915
		3	2.190	0.900	1.805	0.909	0.780	0.923
	50[80%]	1	1.965	0.910	1.774	0.918	0.751	0.928
		2	1.887	0.913	1.730	0.920	0.739	0.932
		3	1.875	0.916	1.702	0.924	0.708	0.936
	80[40%]	1	1.819	0.919	1.492	0.927	0.569	0.941
		2	1.593	0.923	1.350	0.931	0.543	0.946
		3	1.371	0.928	1.234	0.936	0.531	0.949
	80[80%]	1	1.340	0.931	1.190	0.939	0.526	0.951
		2	1.275	0.932	1.131	0.943	0.514	0.953
		3	1.181	0.935	1.060	0.947	0.494	0.956
(2,5)	50[40%]	1	3.166	0.865	1.947	0.889	0.849	0.904
		2	2.814	0.884	1.891	0.891	0.822	0.909
		3	2.219	0.896	1.885	0.904	0.802	0.916
	50[80%]	1	1.979	0.905	1.790	0.913	0.781	0.924
		2	1.946	0.909	1.776	0.914	0.757	0.927
		3	1.885	0.912	1.717	0.917	0.712	0.931
	80[40%]	1	1.851	0.914	1.392	0.922	0.648	0.937
		2	1.609	0.918	1.357	0.928	0.585	0.941
		3	1.380	0.923	1.296	0.931	0.536	0.946
	80[80%]	1	1.359	0.925	1.226	0.933	0.531	0.947
		2	1.347	0.927	1.194	0.937	0.521	0.950
		3	1.188	0.933	1.145	0.940	0.510	0.954

Table 8. The ACLs (1^{st} column) and CPs (2^{nd} column), of 95% ACI/HPD intervals of $R(t)$.

(T_1, T_2)	n[FP%]	Scheme	ACI		HPD			
Prior →					P1		P2	
(1,2)	50[40%]	1	0.288	0.937	0.136	0.949	0.083	0.960
		2	0.283	0.938	0.133	0.950	0.080	0.962
		3	0.276	0.940	0.127	0.952	0.077	0.964
	50[80%]	1	0.230	0.943	0.125	0.953	0.066	0.967
		2	0.228	0.944	0.122	0.954	0.057	0.969
		3	0.225	0.944	0.119	0.956	0.054	0.970
	80[40%]	1	0.221	0.946	0.115	0.957	0.053	0.970
		2	0.219	0.947	0.113	0.959	0.051	0.972
		3	0.216	0.949	0.112	0.960	0.049	0.973
	80[80%]	1	0.180	0.952	0.110	0.962	0.046	0.975
		2	0.179	0.953	0.109	0.963	0.045	0.976
		3	0.170	0.955	0.108	0.963	0.042	0.977
(2,5)	50[40%]	1	0.279	0.940	0.133	0.951	0.081	0.960
		2	0.276	0.941	0.126	0.952	0.078	0.963
		3	0.269	0.943	0.125	0.952	0.073	0.964
	50[80%]	1	0.226	0.946	0.123	0.955	0.059	0.968
		2	0.225	0.947	0.121	0.956	0.053	0.970
		3	0.224	0.947	0.118	0.958	0.052	0.971
	80[40%]	1	0.216	0.949	0.115	0.959	0.051	0.971
		2	0.214	0.950	0.113	0.960	0.049	0.973
		3	0.211	0.951	0.110	0.962	0.047	0.974
	80[80%]	1	0.178	0.953	0.105	0.964	0.044	0.976
		2	0.177	0.953	0.102	0.965	0.042	0.977
		3	0.169	0.955	0.099	0.963	0.037	0.979

Table 9. The ACLs (1^{st} column) and CPs (2^{nd} column), of 95% ACI/HPD intervals of $h(t)$.

(T_1, T_2)	n[FP%]	Scheme	ACI		HPD			
Prior →					P1		P2	
(1,2)	50[40%]	1	1.060	0.918	0.466	0.936	0.139	0.949
		2	0.969	0.920	0.419	0.940	0.136	0.950
		3	0.899	0.924	0.385	0.945	0.132	0.952
	50[80%]	1	0.822	0.929	0.348	0.948	0.131	0.953
		2	0.730	0.935	0.324	0.951	0.129	0.958
		3	0.684	0.939	0.312	0.953	0.125	0.960
	80[40%]	1	0.605	0.944	0.300	0.955	0.123	0.962
		2	0.581	0.946	0.291	0.957	0.120	0.963
		3	0.532	0.949	0.244	0.961	0.119	0.964
	80[80%]	1	0.468	0.954	0.239	0.963	0.115	0.967
		2	0.454	0.956	0.216	0.967	0.112	0.969
		3	0.442	0.958	0.198	0.969	0.110	0.974
(2,5)	50[40%]	1	0.945	0.921	0.454	0.937	0.137	0.951
		2	0.852	0.926	0.392	0.943	0.134	0.952
		3	0.790	0.930	0.372	0.947	0.130	0.954
	50[80%]	1	0.731	0.934	0.361	0.950	0.129	0.958
		2	0.642	0.940	0.293	0.953	0.128	0.960
		3	0.600	0.945	0.286	0.955	0.124	0.962
	80[40%]	1	0.549	0.951	0.263	0.958	0.122	0.964
		2	0.532	0.953	0.247	0.960	0.121	0.967
		3	0.525	0.955	0.226	0.962	0.117	0.968
	80[80%]	1	0.442	0.961	0.208	0.966	0.113	0.970
		2	0.428	0.963	0.189	0.968	0.110	0.973
		3	0.407	0.966	0.176	0.971	0.108	0.976

6. Optimal PT2C designs

In the philosophy of reliability, a researcher aims to choose the best PT2C design among all possible censoring designs to gather the most data about the unknown parameter(s) being investigated. For the first time, [33] discussed the challenge of determining the best censoring. Many different ways of deciding what is best have been suggested, and many different studies have been done on finding the best censoring systems. When the experimenter assigns the values of n, m, and $T_i,\ i = 1, 2$, the ideal PT2C design $\underline{S}$ can be easily determined. According to [34], the best PT2C plan is specified based on the availability of resources, the facilities for experiments, and the importance of cost; see, for example, [35–37], among others. In this study, Table 10 provides three metrics (say $\mathsf{O}_i,\ i = 1, 2, 3$) to assist us in providing the ideal PT2C system.

Table 10. Three optimum criteria for the best PT2C plan.

Criterion	Goal
O_1	Maximize $trace(\mathbf{I}(\hat{\gamma}, \hat{\delta}))$
O_2	Minimize $trace(\mathbf{I}^{-1}(\hat{\gamma}, \hat{\delta}))$
O_3	Minimize $det(\mathbf{I}^{-1}(\hat{\gamma}, \hat{\delta}))$

Obviously, it should be noted that the best PT2C strategies should correspond to the highest (lowest) value of O_1 ($\mathsf{O}_i,\ i = 2, 3$).

7. Physical applications

This part studies three sets of actual data from the physical field to determine if the suggested estimating methods are accurate, useful, and relevant to real-world circumstances. These applications demonstrated that the suggested inferential procedures perform well when applied to real-world data utilizing the proposed strategy.

7.1. Carbon fibers

In this application, we consider a dataset representing the tensile strength of 69 carbon fibers, measured in gigapascals (GPa), tested under tension at gauge lengths of 20 mm; see Table 11. This dataset was first reported by [38] and reanalyzed by [39] and [40].

Table 11. Tensile strength of 69 carbon fibers.

1.312	1.314	1.479	1.552	1.700	1.803	1.861	1.865	1.944	1.958
1.966	1.997	2.006	2.021	2.027	2.055	2.063	2.098	2.140	2.179
2.224	2.240	2.253	2.270	2.272	2.274	2.301	2.301	2.359	2.382
2.382	2.426	2.434	2.435	2.478	2.490	2.511	2.514	2.535	2.554
2.566	2.570	2.586	2.629	2.633	2.642	2.648	2.684	2.697	2.726
2.770	2.773	2.800	2.809	2.818	2.821	2.848	2.880	2.954	3.012
3.067	3.084	3.090	3.096	3.128	3.233	3.433	3.585	3.585	

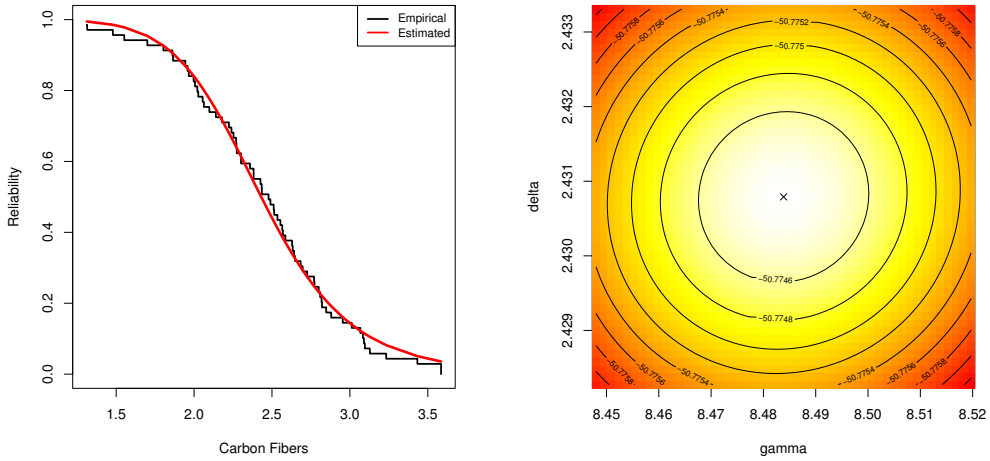

Figure 4. Reliability (left) and contour (right) from tensile strength data.

To show whether the given tensile strength data fit the proposed LogL(γ, δ) distribution or not, the Kolmogorov–Smirnov (K–S) distance (in addition to its P-value) is computed. However, from Table 11, we have the MLEs (with their standard-errors (St-Ers)) of γ and δ as 2.7879(0.4215) and 1.4407(0.1653), respectively; meanwhile, the K–S (P-value) is 0.0741(0.9965). Hence, the LogL lifetime model fits the tensile strength dataset quite well. Moreover, from graphical visualization, Figure 4 displays (i) estimated and empirical LogL reliability $R(t)$ function and (ii) contour diagrams. It

supports the same goodness-of-fit findings and shows that the acquired MLEs $\hat{\gamma} \cong 2.788$ and $\hat{\delta} \cong 1.441$ exist and are unique.

From tensile strength data (for $m = 39$), three artificial G-T2-PHC samples (denoted by S_i, $i = 1, 2, 3,$) are generated; see Table 12. For each sample in Table 12, the point estimates (in addition to their St-Ers) and the 95% interval estimates (in addition to their interval widths (IWs)) of γ, δ, $R(t)$, or $h(t)$ (at mission time $t = 2$) are obtained; see Table 13. Clearly, because there is no prior information regarding γ and δ from the tensile strength dataset, the Bayes point/interval estimations are assessed using incorrect gamma priors by running the MCMC sampler 50,000 times and skipping the first 10,000 of those as burn-in. It is noted from Table 13 that the estimations developed from the Bayes' paradigm of γ, δ, $R(t)$ and $h(t)$ behaved better than others. Figure 5 supports the estimation results reported in Table 13.

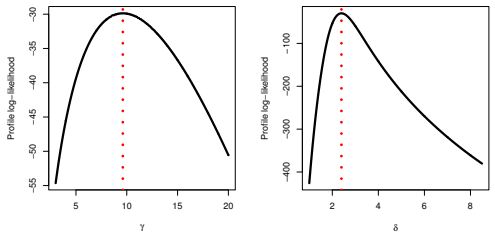

(a) Sample S_1

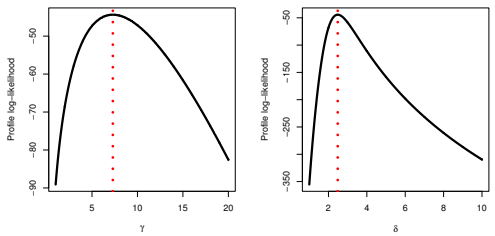

(b) Sample S_2

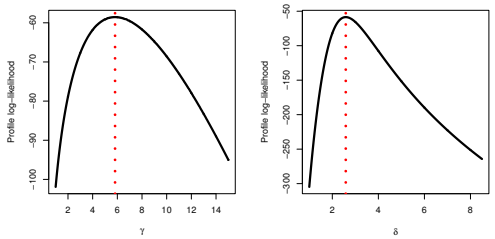

(c) Sample S_3

Figure 5. The log-likelihoods of γ and δ from tensile strength data.

Table 12. Three G-T2-PHC samples from tensile strength data.

S_i	$\underline{\mathsf{S}}$	$T_1(d_1)$	$T_2(d_2)$	S^*	T^*	Data
S_1	$\left(3^{10}, 0^{29}\right)$	1.95(6)	2.75(33)	6	2.75	1.312, 1.314, 1.700, 1.861, 1.865, 1.944, 1.958, 1.997, 2.006, 2.021, 2.027, 2.055, 2.179, 2.224, 2.240, 2.253, 2.270, 2.272, 2.274, 2.301, 2.426, 2.490, 2.511, 2.514, 2.535, 2.554, 2.586, 2.629, 2.633, 2.642, 2.648, 2.684, 2.697
S_2	$\left(0^{14}, 3^{10}, 0^{15}\right)$	2.01(13)	2.65(30)	9	2.65	1.312, 1.314, 1.479, 1.552, 1.700, 1.803, 1.861, 1.865, 1.944, 1.958, 1.966, 1.997, 2.006, 2.021, 2.027, 2.063, 2.098, 2.179, 2.224, 2.240, 2.272, 2.301, 2.301, 2.359, 2.382, 2.554, 2.566, 2.570, 2.586, 2.642
S_3	$\left(0^{29}, 3^{10}\right)$	2.05(15)	2.95(37)	8	2.85	1.312, 1.314, 1.479, 1.552, 1.700, 1.803, 1.861, 1.865, 1.944, 1.958, 1.966, 1.997, 2.006, 2.021, 2.027, 2.055, 2.063, 2.098, 2.140, 2.179, 2.224, 2.240, 2.253, 2.270, 2.272, 2.274, 2.301, 2.301, 2.359, 2.382, 2.426, 2.490, 2.554, 2.629, 2.633, 2.642, 2.848

Table 13. Estimates of γ, δ, $R(t)$, and $h(t)$ from tensile strength data.

Sample	Par.	MLE		MCMC		ACI			HPD		
		Est.	St-Er	Est.	St-Er	Low.	Upp.	IW	Low.	Upp.	IW
S_1	γ	9.6114	1.2911	9.5086	0.1448	7.0809	12.1419	5.0609	9.3107	9.7080	0.3973
	δ	2.3968	0.0660	2.3701	0.0588	2.2673	2.5262	0.2588	2.2666	2.4732	0.2066
	$R(2)$	0.8506	0.0401	0.8317	0.0351	0.7719	0.9293	0.1574	0.7713	0.8862	0.1149
	$h(2)$	0.7179	0.1590	0.8003	0.1625	0.4063	1.0295	0.6232	0.5429	1.0879	0.5451
S_2	γ	7.2915	1.1360	7.1909	0.1414	5.0649	9.5181	4.4532	6.9876	7.3798	0.3922
	δ	2.4825	0.0879	2.4447	0.0725	2.3104	2.6547	0.3444	2.3250	2.5656	0.2406
	$R(2)$	0.8286	0.0394	0.8071	0.0357	0.7514	0.9059	0.1545	0.7509	0.8609	0.1100
	$h(2)$	0.6248	0.1249	0.6934	0.1227	0.3799	0.8696	0.4896	0.5034	0.8984	0.3950
S_3	γ	5.8159	0.8238	5.7143	0.1420	4.2013	7.4305	3.2292	5.5120	5.9029	0.3910
	δ	2.5847	0.1029	2.5356	0.0846	2.3829	2.7864	0.4035	2.4041	2.6726	0.2686
	$R(2)$	0.8163	0.0397	0.7936	0.0343	0.7384	0.8942	0.1557	0.7422	0.8426	0.1004
	$h(2)$	0.5342	0.0976	0.5896	0.0914	0.3430	0.7254	0.3825	0.4497	0.7313	0.2816

Using Sample S_1 (as an example), Figure 6 displays both the density and trace plots of γ, δ, $R(t)$, and $h(t)$. For discrimination, for each sub-plot in Figure 6, the solid and dashed horizontal lines represent the Bayes' and 95% HPD interval estimates, respectively. Figure 6 shows that the recommended MCMC approach clearly converges favorably.

To specify the best censoring $\underline{\mathsf{S}}$ design used in the presence of tensile strength data, utilizing Table 12, the suggested optimum metrics O_i, $i = 1, 2, 3$, provided in Section 6 are computed; see Table 14. It shows, for all given criteria O_i, $i = 1, 2, 3$, that the censoring $\underline{\mathsf{S}} = \left(0^{29}, 3^{10}\right)$ used in Sample S_3 is the optimum plan than others. It also supports the same censoring design recommended in Monte Carlo simulations.

Table 14. The optimum PT2C strategy from tensile strength data.

Sample	O_1	O_2	O_3
S_1	104.4356	1.67125	0.00697
S_2	154.1878	1.29829	0.00842
S_3	239.6767	0.68922	0.00660

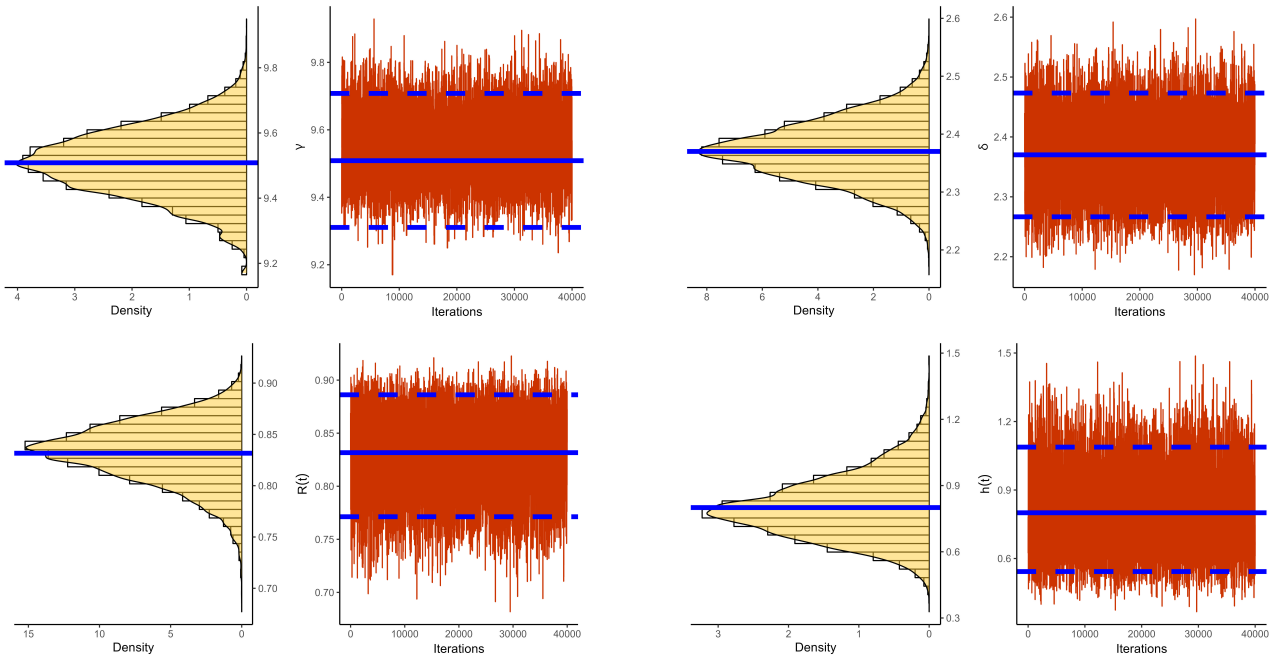

Figure 6. The density and trace diagrams of γ, δ, $R(t)$, and $h(t)$ from tensile strength data.

7.2. Rainfall

This application looks at data collected in the real world. It includes 30 numbers that represent how much rain fell in Minneapolis-Saint Paul (MSP) in March; see Table 15. This dataset was originally provided by [41] and later reanalyzed by [42–44].

Table 15. Consecutive values (in inches) of MSP data.

0.77	1.74	0.81	1.20	1.95	1.20	0.47	1.43	3.37	2.20
3.00	3.09	1.51	2.10	0.52	1.62	1.31	0.32	0.59	0.81
2.81	1.87	1.18	1.35	4.75	2.48	0.96	1.89	0.90	2.05

First, we need to check the fit of the LogL model to the complete MSP data. So, from Table 15, the MLEs (with their St-Ers) of γ and δ are 8.4838(0.8531) and 2.4307(0.0598), respectively, while the K-S statistic (with its P-value) is 0.0480(0.9974). It means that the LogL lifetime model fits the MSP data satisfactorily. Figure 7 indicated that the LogL model is more suitable for the full MSP data as well as that the MLEs $\hat{\gamma} \cong 8.4838$ and $\hat{\delta} \cong 2.4307$ existed and are unique. Here, we proposed taking the estimates $\hat{\gamma}$ and $\hat{\delta}$ as initial guesses.

To evaluate the estimators of γ, δ, $R(t)$, and $h(t)$, three artificial G-T2-PHC samples (when $m = 15$) are obtained from the MSP data; see Table 16. Using it, the estimates of γ, δ, $R(t)$, and $h(t)$ (at $t = 5$) are evaluated; see Table 17. Just like the Bayesian analysis scenario discussed in Subsection 7.1, the Bayes MCMC as well as 95% HPD interval estimates are developed. Thus, from Table 17, the estimates of γ, δ, $R(t)$, and $h(t)$ exhibit the same behavior because they seem to be similar. Figure 8 shows the same outcomes in Table 17. It also highlights the existence and uniqueness of $\hat{\gamma}$ and $\hat{\delta}$.

Figure 9 confirms the same facts presented in Figure 6. Table 18 shows that the censoring $\underline{S} = \left(0^{10}, 3^5\right)$ (in Sample S_3) is better than others. The ideal PT2C process provided here supports the same findings in Section 5 also.

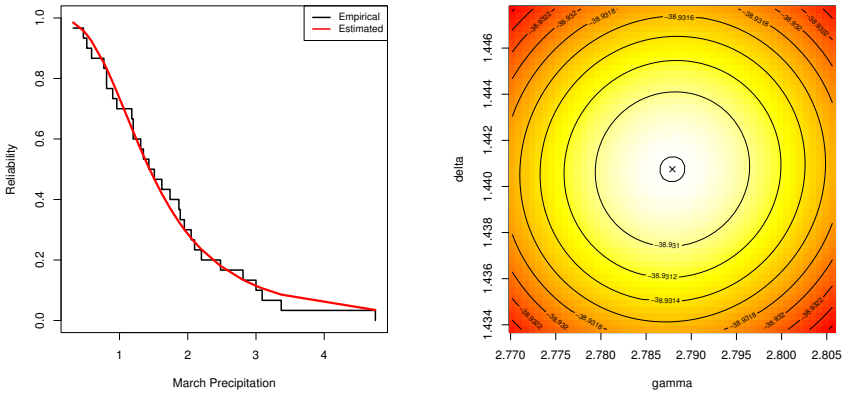

Figure 7. Reliability (left) and contour (right) from MSP data.

Table 16. Various G-T2-PHC samples from MSP data.

S_i	$\underline{S}$	$T_1(d_1)$	$T_2(d_2)$	R^*	T^*	Data
S_1	$\left(3^5, 0^{10}\right)$	0.85(5)	2.05(12)	3	2.05	0.32, 0.47, 0.59, 0.77, 0.81, 0.96, 1.18, 1.20, 1.31, 1.51, 1.74, 1.95
S_2	$\left(0^5, 3^5, 0^5\right)$	0.75(4)	1.25(9)	9	1.25	0.32, 0.47, 0.52, 0.59, 0.77, 0.81, 0.81, 0.96, 1.18
S_3	$\left(0^{10}, 3^5\right)$	0.95(8)	1.55(13)	8	1.55	0.32, 0.47, 0.52, 0.59, 0.77, 0.81, 0.81, 0.90, 0.96, 1.18, 1.20, 1.35, 1.43

Table 17. Estimates of γ, δ, $R(t)$, and $h(t)$ from MSP data.

Sample	Par.	MLE		MCMC		ACI			HPD		
		Est.	St-Er	Est.	St-Er	Low.	Upp.	IW	Low.	Upp.	IW
S_1	γ	2.8717	0.6265	1.6437	4.0997	2.4559	2.7723	0.1396	2.5860	2.9707	0.3847
	δ	1.3456	0.2024	0.9488	1.7423	0.7935	1.2644	0.1189	1.1014	1.4368	0.3354
	$R(1)$	0.7011	0.0875	0.5296	0.8725	0.3429	0.6544	0.0638	0.5667	0.7339	0.1672
	$h(1)$	0.8585	0.2911	0.2880	1.4290	1.1410	0.9578	0.1570	0.7241	1.1911	0.4670
S_2	γ	2.3497	0.6942	0.9891	3.7102	2.7211	2.2508	0.1396	2.0639	2.4503	0.3864
	δ	1.5438	0.3301	0.8968	2.1908	1.2939	1.4551	0.1279	1.2791	1.6321	0.3530
	$R(1)$	0.7350	0.0771	0.5840	0.8861	0.3021	0.6975	0.0487	0.6368	0.7560	0.1192
	$h(1)$	0.6226	0.2608	0.1115	1.1337	1.0222	0.6802	0.0903	0.5509	0.8176	0.2667
S_3	γ	2.2517	0.5494	1.1749	3.3284	2.1535	2.1526	0.1392	1.9659	2.3493	0.3833
	δ	1.5922	0.2738	1.0555	2.1289	1.0734	1.5034	0.1276	1.3275	1.6794	0.3519
	$R(1)$	0.7403	0.0701	0.6028	0.8777	0.2749	0.7047	0.0456	0.6499	0.7604	0.1105
	$h(1)$	0.5848	0.1833	0.2256	0.9441	0.7185	0.6349	0.0784	0.5221	0.7535	0.2315

Table 18. The optimum PT2C strategy from MSP data.

Sample	O_1	O_2	O_3
S_1	20.1190	0.59082	0.03256
S_2	18.1473	0.43351	0.01873
S_3	29.4698	0.37680	0.01471

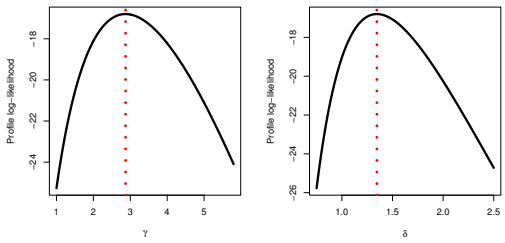

(a) Sample S_1

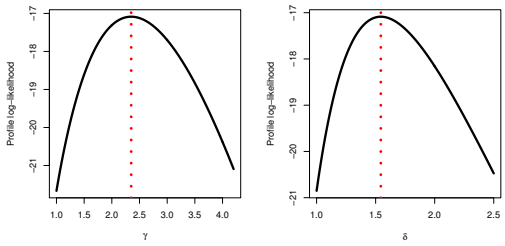

(b) Sample S_2

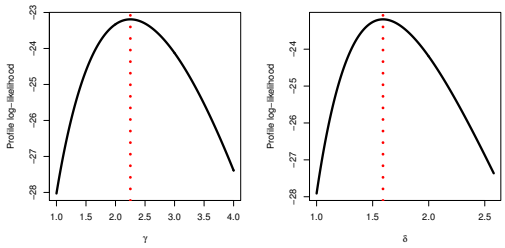

(c) Sample S_3

Figure 8. The log-likelihoods of γ and δ from MSP data.

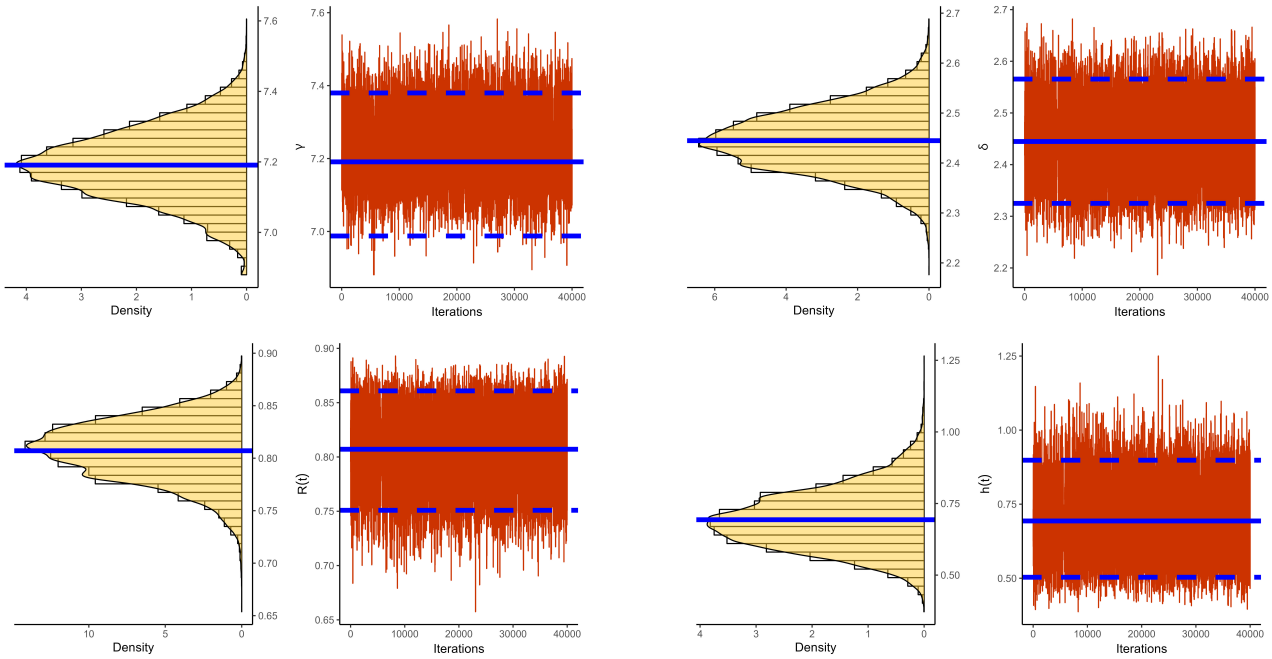

Figure 9. The density and trace diagrams of γ, δ, $R(t)$, and $h(t)$ from MSP data.

7.3. Automobile

This application illustrates a life dataset that represents the losses (of 32 items) from vehicle insurance coverage for private passengers (VIC-PP) in the United Kingdom, given by [45]; see Table 19.

Table 19. The losses from VIC-PP data in UK.

5	21	23	40	44	63	92	96	123	129	140
151	162	166	169	171	245	260	266	304	312	318
343	361	381	448	479	504	578	719	859	970	

First, we need to see if the proposed LogL model matches the complete VIC-PP data. So, according to Table 19, the estimates of $\hat{\gamma}$ and $\hat{\delta}$ (with their St-Ers) are 1.6015(0.2386) and 196.66(37.498), respectively, and the K-S statistic (with its P-value) is 0.0909(0.9319). This means that the LogL model fits the VIC-PP dataset adequately. Figure 10 emphasized that results of $\hat{\gamma}$ and $\hat{\delta}$ exist and are unique. Here, we suggest using the estimates $\hat{\gamma} \cong 1.6015$ and $\hat{\delta} \cong 196.66$ as starting points for any future calculations.

To see how well our estimated values for γ, δ, $R(t)$, and $h(t)$ work, from Table 19, we created three sets of data; see 20. In Table 21, we evaluate the estimates of γ, δ, $R(t)$, and $h(t)$ (at $t = 5$). Similar to the Bayesian analysis scenario mentioned in Subsections 7.1 and 7.2, the Bayes MCMC method and 95% HPD interval estimates are created. From Table 17, we can see that the findings of γ, δ, $R(t)$, or $h(t)$ all show similar patterns as they are close in value to each other. We come to the same conclusion when comparing the asymptotic and highest posterior density interval estimates. Figure 11 confirms

the findings in Table 21 and proves that the estimates of γ and δ exist and are unique.

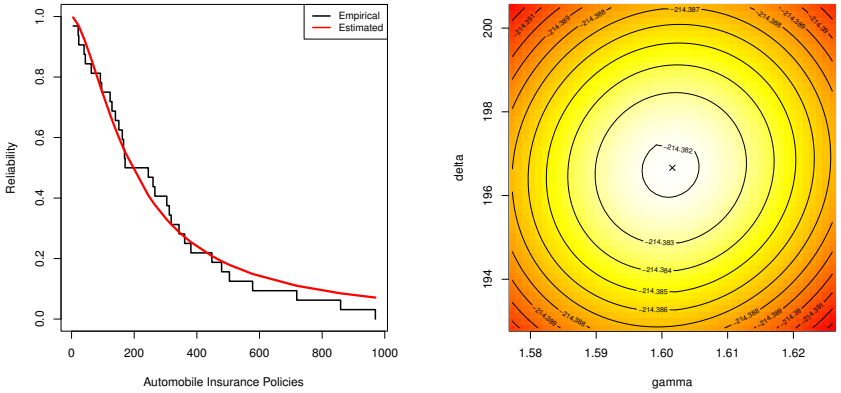

Figure 10. Reliability (left) and contour (right) from VIC-PP data.

Table 20. Various G-T2-PHC samples from VIC-PP data.

S_i	$\underline{S}$	$T_1(d_1)$	$T_2(d_2)$	S^*	T^*	Data
S_1	$\left(4^4, 0^{12}\right)$	350(18)	370(18)	2	350	5, 21, 40, 44, 63, 92, 96, 123, 129, 140, 151, 169, 171, 245, 266, 304, 318, 343
S_2	$\left(0^6, 4^4, 0^6\right)$	80(6)	400(16)	0	381	5, 21, 23, 40, 44, 63, 92, 129, 140, 162, 169, 245, 266, 318, 343, 381
S_3	$\left(0^{12}, 4^4\right)$	50(5)	250(15)	5	250	5, 21, 23, 40, 44, 63, 92, 96, 123, 129, 140, 151, 162, 171, 245

Table 21. Estimates of γ, δ, $R(t)$, and $h(t)$ from VIC-PP data.

Sample	Par.	MLE		MCMC		ACI			HPD		
		Est.	St-Er	Est.	St-Er	Low.	Upp.	IW	Low.	Upp.	IW
S_1	γ	1.4030	0.2684	0.8770	1.9290	1.0520	1.3099	0.1312	1.1262	1.4897	0.3635
	δ	210.78	8.4272	194.26	227.30	33.034	210.68	0.1443	210.48	210.88	0.3941
	$R(50)$	0.8827	0.0398	0.8047	0.9608	0.1562	0.8673	0.0217	0.8364	0.8961	0.0597
	$h(50)$	0.0033	0.0005	0.0023	0.0043	0.0020	0.0034	0.0002	0.0031	0.0037	0.0006
S_2	γ	1.5184	0.3111	0.9087	2.1282	1.2196	1.4217	0.1353	1.2414	1.6136	0.3722
	δ	205.85	8.4404	189.31	222.39	33.086	205.75	0.1440	205.55	205.94	0.3933
	$R(50)$	0.8956	0.0409	0.8153	0.9758	0.1605	0.8813	0.0200	0.8541	0.9086	0.0545
	$h(50)$	0.0032	0.0006	0.0020	0.0044	0.0024	0.0033	0.0002	0.0030	0.0037	0.0007
S_3	γ	1.1944	0.2560	0.6927	1.6961	1.0034	1.1019	0.1304	0.9177	1.2793	0.3617
	δ	240.01	8.3925	223.56	256.46	32.898	239.91	0.1442	239.71	240.11	0.3938
	$R(50)$	0.8669	0.0464	0.7759	0.9579	0.1820	0.8482	0.0263	0.8149	0.8871	0.0722
	$h(50)$	0.0032	0.0004	0.0023	0.0040	0.0017	0.0033	0.0002	0.0031	0.0035	0.0005

Figure 12 indicates that the MCMC technique demonstrates its efficiency by achieving a satisfactory outcome for all unknown quantities. Furthermore, Table 22 shows how the VIC-PP data helps decide the best PT2C plan. This means that using the removal design $\left(0^{12}, 4^4\right)$ in Sample S_3 is the best plan compared to other plans. The best censoring mentioned here aligns with the same ideal censoring developed in Section 5.

Table 22. The optimum PT2C strategy from VIC-PP data.

Sample	O_1	O_2	O_3
S_1	14.0261	71.0890	5.0683
S_2	10.4734	71.3367	6.8112
S_3	15.2909	70.4998	4.6106

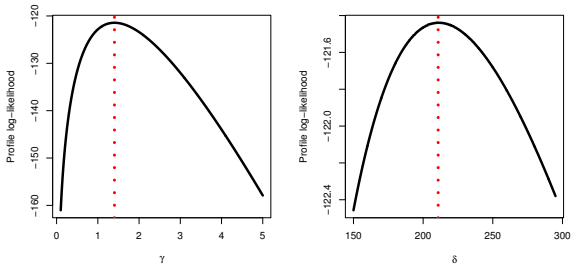

(a) Sample S_1

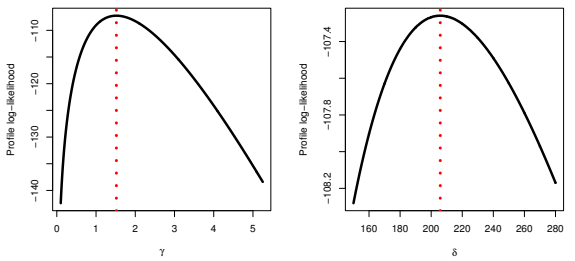

(b) Sample S_2

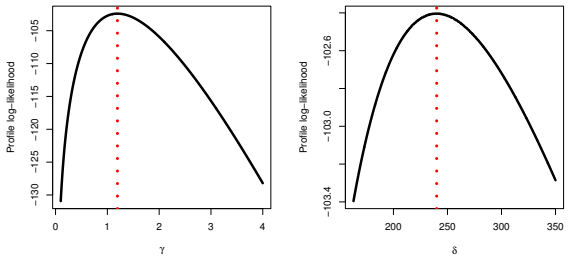

(c) Sample S_3

Figure 11. The log-likelihoods of γ and δ from VIC-PP data.

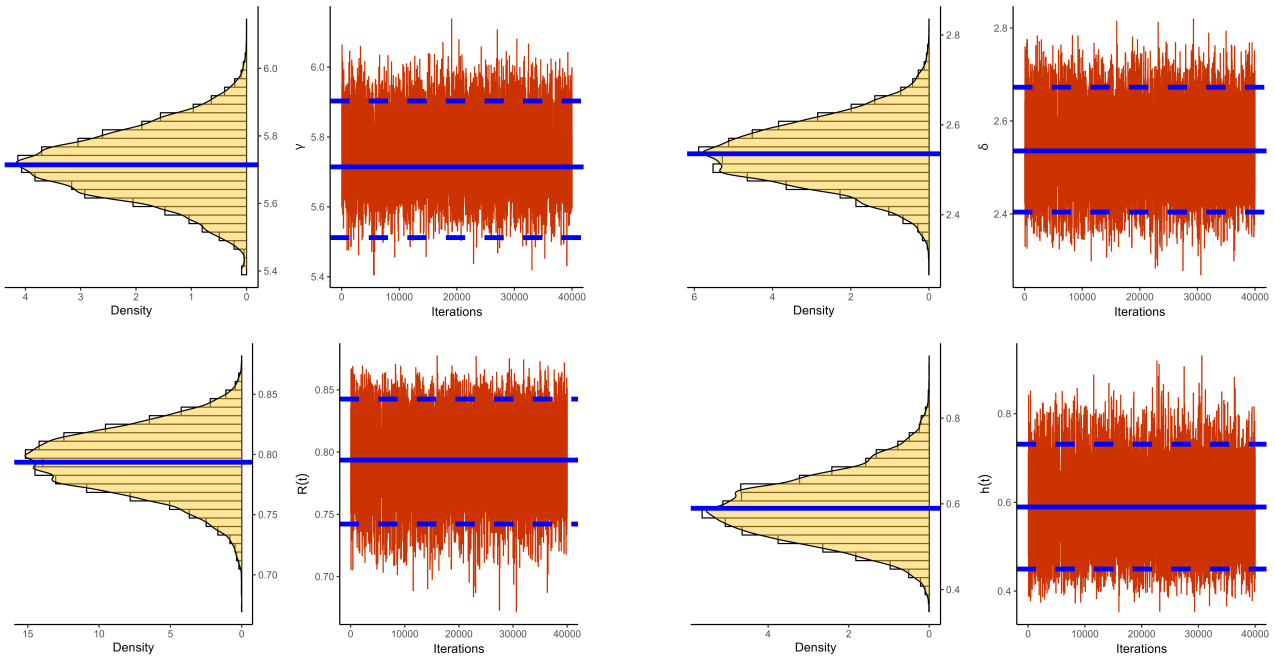

Figure 12. The density and trace diagrams of γ, δ, $R(t)$, and $h(t)$ from VIC-PP data.

8. Concluding remarks

This paper provides several inferential analyses for various parameters of the log-logistic model when samples are generated from the proposed censored strategy. The Newton-Raphson iterative technique has been utilized to obtain the maximum likelihood with their asymptotic interval estimates for all unknown subjects. Additionally, the symmetric Bayes' and associated HPD interval estimates have also been calculated using the Metropolis-Hastings sampler. Numerous simulation experiments have been conducted to compare the acquired estimates. The numerical findings can be summarized as follows:

- Bayesian estimates, especially those using informative gamma priors and the M-H sampler, generally outperformed MLEs in terms of lower RMSE, MRAB, and shorter ACLs, while maintaining high CPs.
- Increasing sample size n or failure percentage (FP%) improved estimation accuracy across all estimators, while greater censoring (i.e., smaller $n - m$) slightly worsened performance.
- Prior-2 (with tighter prior variance) led to more efficient estimates than Prior-1, especially when combined with Scheme-3 (right-censoring), which showed the best performance across all parameter estimates.
- Convergence diagnostics (ACF, BGR, trace plots) confirmed that the MCMC chains mixed well, and the posterior estimates were stable and reliable.
- Optimal PT2C designs were evaluated using criteria based on Fisher information, and the best designs minimized the inverse trace or determinant, leading to more informative experiments.
- Three physics datasets on carbon fiber tensile strength, Minneapolis-Saint Paul rainfall, and vehicle losses demonstrated the utility of the model, showing good fit through K-square tests and

showing that Bayesian estimates provided better results compared to MLEs based on different synthetic censoring scenarios.
- We think that the information and methods discussed in this study will be helpful for researchers and statisticians.

Author contributions

Heba S. Mohammed: Funding acquisition (equal); Methodology (equal); Writing–original draft (equal); Writing–review & editing (equal); Osama E. Abo-Kasem: Methodology (equal); Project administration; Writing–original draft (equal); Ahmed Elshahhat: Methodology (equal); Data curation (equal); Software (equal); Writing–original draft (equal). All authors have read and agreed to the published version of the manuscript.

Use of AI tools declaration

The authors declare they have not used Artificial Intelligence (AI) tools in the creation of this article.

Funding

This research was funded by the Princess Nourah bint Abdulrahman University Researchers Supporting Project number (PNURSP2025R175), Princess Nourah bint Abdulrahman University, Riyadh, Saudi Arabia.

Acknowledgments

The authors would like to express their full thanks to Princess Nourah bint Abdulrahman University, Riyadh, Saudi Arabia, for supporting (PNURSP2025R175) this work.

Conflict of interest

The authors declare that they have no conflicts of interest.

References

1. N. Balakrishnan, E. Cramer, *The Art of Progressive Censoring*, New York: Birkhäuser, 2014. http://doi.org/10.1007/978-0-8176-4807-7
2. D. Kundu, A. Joarder, Analysis of Type-II progressively hybrid censored data, *Comput. Stat. Data Anal.*, **50** (2006), 2509–2528. http://doi.org/10.1016/j.csda.2005.03.007
3. A. Childs, B. Chandrasekar, N. Balakrishnan, Exact likelihood inference for an exponential parameter under progressive hybrid censoring schemes, In: *Statistical Models and Methods for Biomedical and Technical Systems*, Boston: Birkhäuser, 2008, 319–330. http://doi.org/10.1007/978-0-8176-4619-6_23

4. K. Lee, H. Sun, Y. Cho, Exact likelihood inference of the exponential parameter under generalized Type II progressive hybrid censoring, *J. Korean Stat. Soc.*, **45** (2016), 123–136. http://doi.org/10.1016/j.jkss.2015.08.003
5. B. Epstein, Truncated life tests in the exponential case, *Ann. Math. Stat.*, **25** (1954), 555–564. http://doi.org/10.1214/aoms/1177728723
6. A. Childs, B. Chandrasekar, N. Balakrishnan, D. Kundu, Exact likelihood inference based on Type-I and Type-II hybrid censored samples from the exponential distribution, *Ann. Inst. Stat. Math.*, **55** (2003), 319–330. http://doi.org/10.1007/BF02517815
7. L. J. Bain, M. Engelhardt, *Statistical Analysis of Reliability and Life-Testing Models*, 2 Eds., New York: Marcel Dekker, 1991.
8. S. Ashour, A. Elshahhat, Bayesian and non-Bayesian estimation for Weibull parameters based on generalized Type-II progressive hybrid censoring scheme, *Pak. J. Stat. Oper. Res.*, **12** (2016), 213–226. http://doi.org/10.18187/pjsor.v12i2.1337
9. S. Ateya, H. Mohammed, Prediction under Burr-XII distribution based on generalized Type-II progressive hybrid censoring scheme, *J. Egypt. Math. Soc.*, **26** (2018), 491–508. http://doi.org/10.21608/joems.2018.3335.1075
10. S. Cho, K. Lee, Exact Likelihood Inference for a Competing Risks Model with Generalized Type II Progressive Hybrid Censored Exponential Data, *Symmetry*, **13** (2021), 887. http://doi.org/10.3390/sym13050887
11. A. Elshahhat, H. S. Mohammed, O. E. Abo-Kasem, Reliability Inferences of the Inverted NH Parameters via Generalized Type-II Progressive Hybrid Censoring with Applications, *Symmetry*, **14** (2022), 2379. http://doi.org/10.3390/sym14112379
12. L. Wang, Y. Zhou, Y. Lio, and Y. M. Tripathi, Inference for Kumaraswamy Distribution under Generalized Progressive Hybrid Censoring, *Symmetry*, **14** (2022), 403. http://doi.org/10.3390/sym14020403
13. A. Elshahhat, H. S. Mohammed, O. E. Abo-Kasem, Statistical Evaluations and Applications for IER Parameters from Generalized Progressively Type-II Hybrid Censored Data, *Axioms*, **12** (2023), 565. http://doi.org/10.3390/axioms12060565
14. A. Elshahhat, O. E. Abo-Kasem, H. S. Mohammed, Statistical Analysis of Type-II Generalized Progressively Hybrid Alpha-PIE Censored Data and Applications in Electronic Tubes and Vinyl Chloride, *Axioms*, **12** (2023), 601. http://doi.org/10.3390/axioms12060601
15. A. Elshahhat, O. E. Abo-Kasem, H. S. Mohammed, Reliability Analysis and Applications of Generalized Type-II Progressively Hybrid Maxwell–Boltzmann Censored Data, *Axioms*, **12** (2023), 618. http://doi.org/10.3390/axioms12070618
16. D. Collet, *Modelling Survival Data in Medical Research*, London: Chapman and Hall, 2003.
17. C. Kus,M. F. Kaya, Estimation of parameters of the log-logistic distribution based on progressive censoring using the EM algorithm, *Hacettepe J. Math. Stat.*, **35** (2006), 203–211.
18. S. Hyun, J. Lee, R. Yearout, Parameter estimation of Type-I and Type-II hybrid censored data from the log-logistic distribution, *Ind. Syst. Eng. Rev.*, **4** (2016), 37–44.

19. Y. Du, Y. Guo, W. Gui, Statistical inference for the information entropy of the log-logistic distribution under progressive type-I interval censoring schemes, *Symmetry*, **10** (2018), 445. http://doi.org/10.3390/sym10100445

20. M. F. Sewailem, A. Baklizi, Inference for the log-logistic distribution based on an adaptive progressive type-II censoring scheme, *Cogent Math. Stat.*, **6** (2019), 1684228. http://doi.org/10.1080/25742558.2019.1684228

21. Y. Xie, W. Gui, Statistical inference of the lifetime performance index with the log-logistic distribution based on progressive first-failure-censored data, *Symmetry*, **12** (2020), 937. http://doi.org/10.3390/sym12060937

22. M. Shrahili, A. R. El-Saeed, A. S. Hassan, I. Elbatal, M. Elgarhy, Estimation of entropy for log-logistic distribution under progressive type II censoring, *J. Nanomater.*, **2022** (2022), 2739606. https://doi.org/10.1155/2022/2739606

23. K. Maiti, S. Kayal, Estimating reliability characteristics of the log-logistic distribution under progressive censoring with two applications, *Ann. Data Sci.*, **10** (2023), 89–128. https://doi.org/10.1007/s40745-020-00292-y

24. S. Dey, A. Elshahhat, M. Nassar, Analysis of progressive type-II censored gamma distribution, *Comput. Stat.*, **38** (2023), 481–508. https://doi.org/10.1007/s00180-022-01239-y

25. A. Gelman, J. B. Carlin, H. S. Stern, D. B. Rubin, *Bayesian Data Analysis*, 2 Eds., USA: Chapman and Hall/CRC, 2004.

26. S. M. Lynch, *Introduction to Applied Bayesian Statistics and Estimation for Social Scientists*, New York: Springer, 2007. http://doi.org/10.1007/978-0-387-71265-9

27. J. F. Lawless, *Statistical Models and Methods for Lifetime Data*, 2 Eds., Hoboken: John Wiley and Sons, 2003.

28. W. H. Greene, *Econometric Analysis*, 4 Eds., New York: Prentice-Hall, 2000.

29. M. H. Chen, Q. M. Shao, Monte Carlo estimation of Bayesian credible and HPD intervals, *J. Comput. Gr. Stat.*, **8** (1999), 69–92. http://doi.org/10.1080/10618600.1999.10474802

30. A. Henningsen, O. Toomet, maxLik: A package for maximum likelihood estimation in R, *Comput. Stat.*, **26** (2011), 443–458. http://doi.org/10.1007/s00180-010-0217-1

31. M. Plummer, N. Best, K. Cowles, K. Vines, CODA: Convergence diagnosis and output analysis for MCMC, *R News*, **6** (2006), 7–11.

32. D. Kundu, Bayesian inference and life testing plan for the Weibull distribution in presence of progressive censoring, *Technometrics*, **50** (2008), 144–154. https://doi.org/10.1198/004017008000000217

33. N. Balakrishnan, R. Aggarwala, *Progressive Censoring: Theory, Methods and Applications*, Boston: Birkhäuser, 2000.

34. H. K. T. Ng, P. S. Chan, N. Balakrishnan, Optimal progressive censoring plans for the Weibull distribution, *Technometrics*, **46** (2004), 470–481. https://doi.org/10.1198/004017004000000482

35. T. Sen, Y. M. Tripathi, R. Bhattacharya, Statistical inference and optimum life testing plans under Type-II hybrid censoring scheme, *Ann. Data Sci.*, **5** (2018), 679–708. https://doi.org/10.1007/s40745-018-0158-z

36. S. K. Ashour, A. A. El-Sheikh, A. Elshahhat, Inferences and optimal censoring schemes for progressively first-failure censored Nadarajah-Haghighi distribution, *Sankhya A*, **84** (2020), 885–923. https://doi.org/10.1007/s13171-019-00175-2

37. A. Elshahhat, W. S. Abu El Azm, Statistical reliability analysis of electronic devices using generalized progressively hybrid censoring plan, *Qual. Reliab. Eng. Int.*, **38** (2022), 1112–1130. https://doi.org/10.1002/qre.3058

38. M. G. Bader, A. M. Priest, Statistical aspects of fibre and bundle strength in hybrid composites, *Prog. Sci. Eng. Compos.*, 1982, 1129–1136.

39. S. V. Singh, V. K. Sharma, S. K. Singh, Inferences for two parameter Teissier distribution in case of fuzzy progressively censored data, *Reliab.: Theory Appl.*, **17** (2022), 559–573.

40. M. Nassar, R. Alotaibi, A. Elshahhat, Bayesian estimation of some reliability characteristics for Nakagami model using adaptive progressive censoring, *Phys. Scr.*, **99** (2024), 095271. http://doi.org/10.1088/1402-4896/ad6f4a

41. D. Hinkley, On quick choice of power transformation, *J. R. Stat. Soc.*, **26** (1977), 67–69.

42. A. Elshahhat, R. Bhattacharya, H. S. Mohammed, Survival Analysis of Type-II Lehmann Fr0̆0e9chet Parameters via Progressive Type-II Censoring with Applications, *Axioms*, **11** (2022), 700. http://doi.org/10.3390/axioms11120700

43. A. Elshahhat, A. H. Muse, O. M. Egeh, B. R. Elemary, Estimation for parameters of life of the Marshall-Olkin generalized-exponential distribution using progressive Type-II censored data, *Complexity*, **2022** (2022), 8155929. https://doi.org/10.1155/2022/8155929

44. R. Alotaibi, M. Nassar, A. Elshahhat, Rainfall data modeling using improved adaptive type-II progressively censored Weibull-exponential samples, *Sci. Rep.*, **14** (2024), 30484. https://doi.org/10.1038/s41598-024-80529-5

45. N. M. Alfaer, A. M. Gemeay, H. M. Aljohani, A. Z. Afify, The extended log-logistic distribution: inference and actuarial applications, *Mathematics*, **9** (2021), 1386. http://doi.org/10.3390/math9121386

AIMS Press